



**Escola de Camins**

Escola Tècnica Superior d'Enginyeria de Camins, Canals i Ports  
UPC BARCELONATECH

# Seismic fragility functions for reinforced concrete walls in low-rise housing

Final Thesis developed by:

Alvarez Gutierrez, Carlos Arturo

Directed by:

Murcia-Delso, Juan

Master in:

Structural and Construction Engineering

Barcelona, July 2023

Department of Civil and Environmental Engineering

**MASTER FINAL THESIS**

## **Acknowledgments**

I would like to express my deepest gratitude and appreciation to the following individuals who have played a significant role in the completion of my master's thesis:

First and foremost, I would like to express my heartfelt gratitude to my parents, Ana and Carlos, for their unwavering love, support, and encouragement throughout my academic and personal journey. Your constant belief in me has been a driving force behind my accomplishments. You have not only been my pillars of strength but also shining examples of hard work, determination, and resilience. Your unwavering dedication to your own pursuits has inspired me to always give my best and strive for excellence. I am truly grateful for the invaluable life lessons you have imparted and for being the guiding lights in my life.

I am also grateful to my brothers, David, Andrea, and Esteban, for their understanding, patience, and encouragement during this challenging period. Your presence and words of encouragement have been invaluable.

To my extended family residing in Mexico, thank you for your continuous support and encouragement. Your love and encouragement from afar have always meant a lot to me.

I extend my heartfelt gratitude to my thesis tutor, Juan Murcia-Delso, for his guidance, expertise, and valuable insights throughout the research process. Your mentorship has been instrumental in shaping the direction of my work, and I am grateful for your patience and dedication.

To my dear friends from Barcelona and Mexico, thank you for your constant support, motivation, and understanding. Your friendship has provided me with strength and solace during both the academic and personal challenges I encountered.

Finally, I would like to express my appreciation to all the individuals who have contributed in ways big and small to the completion of this thesis. Your support, advice, and encouragement have made a significant impact on my academic journey.

To each and every person mentioned above, and to all those who have supported me along the way, I offer my sincerest thanks. Your belief in me and your unwavering support have been invaluable, and I am deeply grateful for your presence in my life.

Barcelona, 26 of june of 2023

## **Abstract**

Seismic events pose significant challenges to the vulnerability of buildings, particularly in low-rise housing structures in Latin America. This study focuses on the development of seismic fragility functions specifically tailored to reinforced concrete walls in low-rise housing. The objective is to analyze the behavior of these walls under seismic forces and evaluate their vulnerability by considering various damage states. Damage State 1 (Slight), Damage State 1 (Moderate), and Damage State 3 (Severe). A comprehensive literature review was conducted, examining relevant studies on fragility functions for reinforced concrete walls. The study incorporates data from laboratory experiments and databases, including "Performance-Based Assessment and Design of Squat Reinforced Concrete Shear Walls." The developed fragility functions capture the relationship between seismic demand (drift ratio) and the performance of reinforced concrete walls, allowing for the assessment of their vulnerability to different damage states. These functions provide valuable insights for designers and engineers, facilitating the development of improved design strategies and retrofit measures. By enhancing the understanding of reinforced concrete walls' response to seismic events, this research contributes to the creation of more resilient and safer low-rise housing structures. The findings aim to minimize economic losses and protect human life in areas prone to seismic activity, ultimately improving the overall resilience of communities.

**Keywords:** fragility functions, reinforced concrete walls, damage states.

## Content

Acknowledgments .....	I
Abstract.....	III
Content .....	IV
List of Figures.....	VI
List of Tables .....	IX
List of Symbols.....	XI
1 Introduction .....	1
1.1 Motivation for the present work .....	1
1.2 Objectives and Scope.....	2
1.3 Guidelines .....	5
2 Review of the state of the art .....	6
2.1 Seismic response of squat walls.....	9
2.2 Damage fragility analysis .....	18
3 Methodology for developing fragility functions .....	26
3.1 Overview.....	26
3.2 Definition of Damage States .....	27
3.2.1 Data Collection.....	37
3.3 Development of fragility functions.....	53
3.3.1 Fragility Function Definition.....	53




---

3.3.2	Derivation of fragility parameters .....	54
4	Results .....	58
4.1	Fragility Functions .....	58
4.1.1	Damage State 1 (Slight).....	58
4.1.2	Damage State 2 (Moderate).....	61
4.1.3	Damage State 3 (Severe) .....	63
4.2	Summary and Discussion.....	66
4.2.1	Comparison with FEMA 356 (2000) drift ratio limits .....	67
4.2.2	Comparison with fragility functions proposed by Gulec et al. (2010) .....	70
5	Conclusions .....	75
5.1	Recommendations for future works.....	77
6	References .....	78

## List of Figures

Figure 1. Configuration of type 1 houses on one level. Source: Carrillo (2010) .....	1
Figure 2. Illustration 40, web crushing. Source: Moreno (2014) .....	2
Figure 3. Component force-deformation behavior, ductility, and severity of damage. Source: FEMA 306.....	10
Figure 4. Specimen B3 at the End of the Test. Source: Oesterle et al. (1979) .....	11
Figure 5. Load-deflection plot for Specimen B3. Source: Oesterle et al. (1979).....	12
Figure 6. Diagonal tension (a) T1-S1, (b) T1-S2, (c) T1-N10-S1. Source: Terzioglu et al. (2018). .....	13
Figure 7. Diagonal compression (d) T2-S. Source: Terzioglu et al. (2018).....	14
Figure 8. Sliding shear (e) T5-S1, (f) T3-S1. Source: Terzioglu et al. (2018).....	15
Figure 9. Reinforcement buckling and fracture observed in wall SWD-1. Source: Bar buckling in ductile RC walls with different boundary zone detailing: Experimental investigation. Tripathi et al. (2018). .....	16
Figure 10. Out-of-plane induced damage in an RC wall after the New Zealand earthquake: Source: Sritharan et al.(2011).....	17
Figure 11. Displacement Parameters for Damage Evaluation. Source: FEMA 306 .....	20
Figure 12. Global displacement demand for undamaged, damaged, and restored/upgraded conditions. Source: FEMA 308 .....	21
Figure 13. Model MCN100D before the test. Source: Carrillo (2010) .....	28
Figure 14. Cracking evolution of Model MCN100D. Source: Carrillo (2010).....	29
Figure 15. Hysteresis curve for specimen 24. Source: Hidalgo .....	36
Figure 16. Hysteresis curve for specimen 30. Source: Hidalgo .....	36
Figure 17. Wall's Height-to-length ratio.....	39

---

Figure 18. Concrete compressive strength of the walls.....	40
Figure 19. Horizontal and vertical (% of $\rho$ min) .....	41
Figure 20. Geometry of square cross-section walls. Source: Carrillo (2010) .....	43
Figure 21. Measured mechanical properties of concrete. Source: Backbone Model for Performance-Based Design of RC Walls for Low-Rise Housing .....	43
Figure 22. Measured mechanical properties of steel reinforcement. Source: Backbone Model for Performance-Based Design of RC Walls for Low-Rise Housing .....	44
Figure 23. Test setups: (a) shake table testing, (b) quasi-static testing. Source: Carrillo & Alcocer.....	46
Figure 24. Performance levels and damage states. Source: Acceptance limits for performance-based seismic design of RC walls for low-rise housing. Carrillo and Alcocer.....	47
Figure 25. Test setup. Source: Hidalgo .....	51
Figure 26. Typical lognormal fragility function (a); and evaluation of individual damage state probabilities (b). Source: FEMA P-58-1 .....	54
Figure 27. Fragility curve for Damage State 1 (Slight).....	60
Figure 28. Fragility curve for Damage State 2 (Moderate) .....	62
Figure 29. Fragility curve for Damage State 3 (Severe).....	65
Figure 30. Fragility curves for DS1 (Cracking), DS2 (Life Safety), DS3 (Peak Shear Strength) .....	67
Figure 31. Modeling Parameters and Numerical Acceptance Criteria for Nonlinear Procedures - Members Controlled by Shear. Source: FEMA 356 (2000).....	68
Figure 32. FEMA 356 Drift values and Probability of exceedance for each Damage State .....	70





---

Figure 33. Damage states and corresponding methods of repair. Source: Fragility functions for low aspect ratio reinforced concrete walls. Gulec et al. (2010)..... 71

Figure 34. Lognormal distribution parameters and the corresponding Lilliefors test results. Source Fragility functions for low aspect ratio reinforced concrete walls. Gulec et al. (2010)..... 71

Figure 35. Fragility functions for rectangular walls. Source: Fragility functions for low aspect ratio reinforced concrete walls. Gulec et al. (2010) ..... 72

---

## List of Tables

Table 1. Component Damage Classification. Source: FEMA 306.....	24
Table 2. Summary of repair procedures. Source: FEMA 308.....	25
Table 3. RC1B Component Damage Classification Guide. Source: FEMA 306.....	32
Table 4. RC1C Component Damage Classification Guide. Source: FEMA 306.....	33
Table 5. Damage States - Seismic fragility functions for reinforced concrete walls in low-rise housing.....	34
Table 6. Wall Identification.....	44
Table 7. Wall's geometrical and mechanical properties. Carrillo and Alcocer .....	45
Table 8. Test results. Carrillo and Alocer.....	48
Table 9. Wall's geometrical and mechanical properties. Hidalgo.....	50
Table 10. Test Results. Hidalgo .....	52
Table 11. Values of R for applying Peirce's Criterion. Source: FEMA-P-58-V1 (2018).....	56
Table 12. Values for Elimination of Outliers .....	56
Table 13. Lilliefors test for Damage States .....	57
Table 14. Story drift ratio for DS1 (Slight) .....	58
Table 15. Fragility parameters for DS1 (Slight).....	60
Table 16. Story drift ratio for DS2 (Moderate) .....	61
Table 17. Fragility parameters for DS2 (Moderate) .....	62
Table 18. Story drift ratio for DS3 (Severe) .....	63



---

Table 19. Fragility parameters for DS3 (Severe) .....	64
Table 20. Lognormal distribution parameters and Lilliefors test .....	66
Table 21. Probability of exceedance for Drift Ratio FEMA 356 .....	68
Table 22. Geometrical properties for squat walls. Source: Gulec (2009) .....	72
Table 23. Wall's mechanical and geometrical properties .....	75
Table 24. Fragility Parameters for Damage States .....	76

## List of Symbols

<b>Symbols</b>	<b>Comment</b>
$\sigma_v$	Axial compressive stress
$f'_c$	Concrete compressive strength
$F_i(D)$	Conditional probability of Damage State exceedance
$\delta_{cr}$	Cracking drift
$V_{cr}$	Cracking shear resistance as per ACI-318
$\mu$	Ductility
$h_w$	Height of the wall
$l_w$	Length of the wall
$\delta_{LS}$	Life Safety drift
$\beta_i$	Logarithmic standard deviation for damage state “i”
$d_c$	Maximum global displacement capacity
$d_d$	Maximum global displacement demand
$V_{max}$	Maximum shear resistance as per ACI-318
$MPa$	Megapascal
$M$	Moment applied to the wall
$\delta_{max}$	Peak shear resistance drift
$\beta_r$	Random variability
$\beta_u$	Represents uncertainty of the tests
$I_{crack}$	Residual crack index
$V$	Shear force applied to the wall
$\theta$	Standard normal (Gaussian)

---

$t_w$	Thickness of the wall
$\rho$	Web steel ratio
$f_y$	Yield stress of reinforcement

# 1 Introduction

## 1.1 Motivation for the present work

In seismic hazard zones, the vulnerability of buildings to earthquakes poses significant challenges. This is particularly evident in low-rise housing (Figure 1), where factors such as limited structural design knowledge, the use of low-cost materials, and self-construction practices can result in structures with low ductile behavior. When subjected to seismic events, these buildings are prone to experiencing severe damage, leading to devastating economic losses and potential threats to human life.



*Figure 1. Configuration of type 1 houses on one level. Source: Carrillo (2010)*

Reinforced concrete shear walls ensure low-rise houses' structural integrity and resilience in areas prone to seismic activity. These walls are designed to resist lateral forces induced by earthquakes and provide stability to the overall structure. The performance of reinforced concrete shear walls can be influenced by various factors given their material and geometrical properties. Due to their relatively low height-to-length ratio, walls in low-rise housing tend to have failures due to shear behavior (Figure 2).



Figure 2. Illustration 40, web crushing. Source: Moreno (2014)

In performance-based seismic design and assessment methods [1], understanding the observed damages in reinforced concrete shear walls becomes essential. These damages serve as critical indicators of the structural response under seismic loading conditions and provide valuable insights into the vulnerabilities and limitations of the walls. Utilizing fragility curves are useful tool for assessing the probable performance and predicting the potential damage levels of reinforced concrete shear walls. Fragility curves provide a probabilistic framework that relates the intensity of seismic demands to the likelihood of exceeding different damage states. These curves allow for a comprehensive understanding of the expected performance of reinforced concrete shear walls and aid in assessing seismic risk, developing appropriate design strategies as well as retrofit measures to enhance their resilience.

## 1.2 Objectives and Scope

The objective of this master's thesis is to develop seismic fragility functions specifically tailored to reinforced concrete walls in low-rise housing in Latin America. By

---

comprehending the behavior of these walls under seismic forces, it becomes possible to analyze their vulnerability to damage and enhance their performance through improved design strategies. This research aims to provide valuable insights to designers and engineers, enabling them to assess the risk of existing constructions. This is particularly critical for areas characterized by self-construction practices and low-cost materials. This will facilitate the implementation of appropriate measures, such as improved designs or retrofit actions, to increase the resilience of communities residing in such structures.

To achieve this goal, an extensive literature review was conducted to characterize the seismic damage response of low-rise reinforced concrete wall construction and a database of relevant wall tests was compiled from the literature. This database contains valuable information about the behavior and performance of squat reinforced concrete shear walls, commonly utilized in low-rise housing constructions.

The primary focus when reviewing these experiments was to investigate the characteristics of reinforced concrete walls, the materials used in their construction, and their response to lateral loading. By studying the outcomes of these experiments, we can extract critical information to develop fragility functions that capture the relationship between seismic demand and damageability of the walls. These fragility functions serve as essential tools for analyzing the behavior of reinforced concrete walls and assessing their vulnerability to seismic actions.

The significance of this research lies in its potential to inform designers and engineers about the expected performance of reinforced concrete walls in low-rise housing when subjected to seismic events. Integrating fragility functions into probabilistic performance-



based assessment processes makes it possible to identify potential weak points and implement appropriate design or retrofit measures to mitigate the risks associated with low-ductile behavior and low-cost materials. Ultimately, this research aims to contribute to developing more resilient and safer housing in areas prone to seismic activity, thereby minimizing economic losses and potential threats to human life.

The evaluation of the seismic performance of reinforced concrete walls in low-rise housing involves the identification of distinct damage states that reflect the severity of structural damage under seismic loading conditions. These damage states include different levels of damage (from slight to severe), with each level (state) corresponding to a specific intensity of repair needs. The behavior of reinforced concrete walls under seismic forces is commonly assessed using a demand parameter known as drift ratio. The drift ratio measures the relative displacement between different levels of a structure caused by lateral movement during an earthquake. It provides a valuable indication of the deformation experienced by the walls and serves as a crucial input for determining the performance level and associated damage states. By analyzing the response of the walls at different levels of drift, valuable insights can be gained into their vulnerability and capacity to withstand seismic forces.

The experimental results from the studies conducted by Carrillo and Alcocer [2] and Hidalgo [3] were utilized in this research, with the characteristics of the walls presented in subsequent sections of this study. These studies provided data for each tested wall, correlating a certain level of damage with the corresponding drift. Guidelines from FEMA 306 and FEMA 308 were employed to define the damage levels. Understanding the potential drift levels induced by earthquake forces on a structure or its components makes

it possible to estimate the probability of exceeding the defined damage levels. The fragility curve herein developed is limited to reinforced concrete walls with characteristics like the ones presented in the experimental studies.

### 1.3 Guidelines

The following guidelines from the Federal Emergency Management Agency (FEMA) and Applied Technology Council (ATC) have been used to develop fragility functions for reinforced concrete shear walls:

- ATC-40: Seismic evaluation and retrofit of concrete buildings. Volume 1.
- FEMA 273: National Earthquake Hazards Reduction Program (NEHRP) – Guidelines for the Seismic Rehabilitation of Buildings.
- FEMA 306: Basic Procedures Manual. Evaluation of Earthquake Damaged Concrete and Masonry Wall Buildings. Prepared by: Applied Technology Council (ATC-43 Project)
- FEMA 307: Technical Resources. Evaluation of Earthquake Damaged Concrete and Masonry Wall Buildings. Prepared by: Applied Technology Council (ATC).
- FEMA 308: Repair of Earthquake Damaged Concrete and Masonry Wall Buildings. Prepared by: Applied Technology Council (ATC).
- FEMA P-58-1: Seismic Performance Assessment of Buildings. Volume 1 – Methodology

---

## 2 Review of the state of the art

Performance-based design procedures involve the evaluation of two essential elements: the seismic demand and seismic capacity. Demand represents the ground motion generated by earthquakes, while capacity refers to a structure's ability to withstand that seismic demand with a maximum pre-defined level of damage. The performance of a structure is determined by how its capacity can respond to the demand, aligning with the design objectives. A structure's capacity is determined by its individual components' strength and deformation capacities. To assess capacities beyond the elastic limits, nonlinear analysis methods like the pushover procedure are utilized. This procedure involves conducting a series of sequential elastic analyses, combining them to create a force-displacement capacity diagram for the overall structure. The pushover process continues until the structure becomes unstable or reaches a predetermined limit. The demand, or displacement, represents the horizontal motion produced by ground motions during an earthquake. Tracking this motion at every time-step for design purposes is impractical. Nonlinear analysis methods simplify the process by using a set of lateral displacements as a design condition. The displacement demand provides an estimate of the maximum expected response of the building during the ground motion. A performance check can be conducted once the capacity curve and displacement demand are defined. This check ensures that both structural and nonstructural components remain within acceptable limits defined by the performance objectives for the forces and displacements indicated by the displacement demand.[4]

---

Although an elastic analysis accurately measures a structure's elastic capacity and identifies the point of first yielding, it cannot predict failure modes or take force redistribution into account during progressive yielding. Inelastic analysis methods help explain how structures work by identifying failure modes and the possibility of gradual collapse. To offer engineers a better understanding of how structures will react during major seismic events where the elastic capacity of the structure is likely to be exceeded, inelastic analysis is employed for design and evaluation. This eliminates some of the uncertainty associated with elastic techniques.

Recently developed guidelines for structural engineering seismic analysis and design techniques focus on building displacement rather than forces as the primary parameter for the characterization of seismic performance. This approach models the building as an assembly of its individual components. Force-deformation properties (e.g., elastic stiffness, yield point, ductility) control the behavior of wall panels, beams, columns, and other members. The component behavior, in turn, governs the overall displacement of the building and its seismic performance. Thus, the evaluation of the effects of damage on building performance must concentrate on how component properties change because of damage. [5]

During an earthquake, reinforced concrete squat walls experience complex seismic responses that are affected by various factors, such as the wall geometry (rectangular, barbell, and flanged), boundary conditions, reinforcement detailing, and loading characteristics. The seismic response of reinforced concrete walls can be evaluated using analytical or numerical models, which consider the dynamic behavior of the wall and its interaction with the surrounding structure.

The analysis and design of most reinforced concrete walls without openings can be treated as a beam-column where lateral forces are introduced by a series of point loads through the floor diaphragms. Given their aspect ratio height-to-length ( $h_w/l_w$ ), slender walls are distinguished with ratios greater than two and squat walls for ratios less than or equal to two. It is important to note that squat walls have high flexural strength, even for minimal vertical reinforcement, so it is necessary to apply very high shear forces to develop such strength. This causes the behavior of this type of wall to be dominated by shear. [6]

Suppressing shear failure in the seismic design is a desirable earthquake-resistant philosophy for reinforced concrete walls. According to experimental studies, tall (or slender) walls that are carefully designed and detailed will yield flexure rather than fail in shear. On the other hand, squat walls are vulnerable to shear failure, often characterized by a rapid loss of strength and stiffness under cyclic loading.

When reinforced concrete walls are subjected to cyclic forces, once the maximum flexural strength of the cross-section is exceeded, the loss of rigidity and residual deformation begins to be significantly higher, even without reaching the exact value of the force.

---

## 2.1 Seismic response of squat walls

Reinforced concrete squat walls are commonly used in low-rise houses as a part of the lateral resistant structure in seismic hazard zones. The behavior of the wall is determined by characteristics such as height-to-length ( $h_w/l_w$ ) ratio, cross-section geometry, and materials concrete compressive strength ( $f'_c$ ) and steel yielding strength ( $f_y$ ). Reinforcement is made of steel deformed bars or welded-wire mesh. The interaction of the wall with the surrounding structure (boundary condition) is another essential condition to determine the behavior of the wall.

The capability of a system or structural element to undergo large amplitude cyclic deformations, under a given ground motion, without excessive strength deterioration is typically provided by the available ductility ratio,  $\mu$ . Some loss of stiffness is inevitable, but excessive stiffness loss can lead to collapse [7].

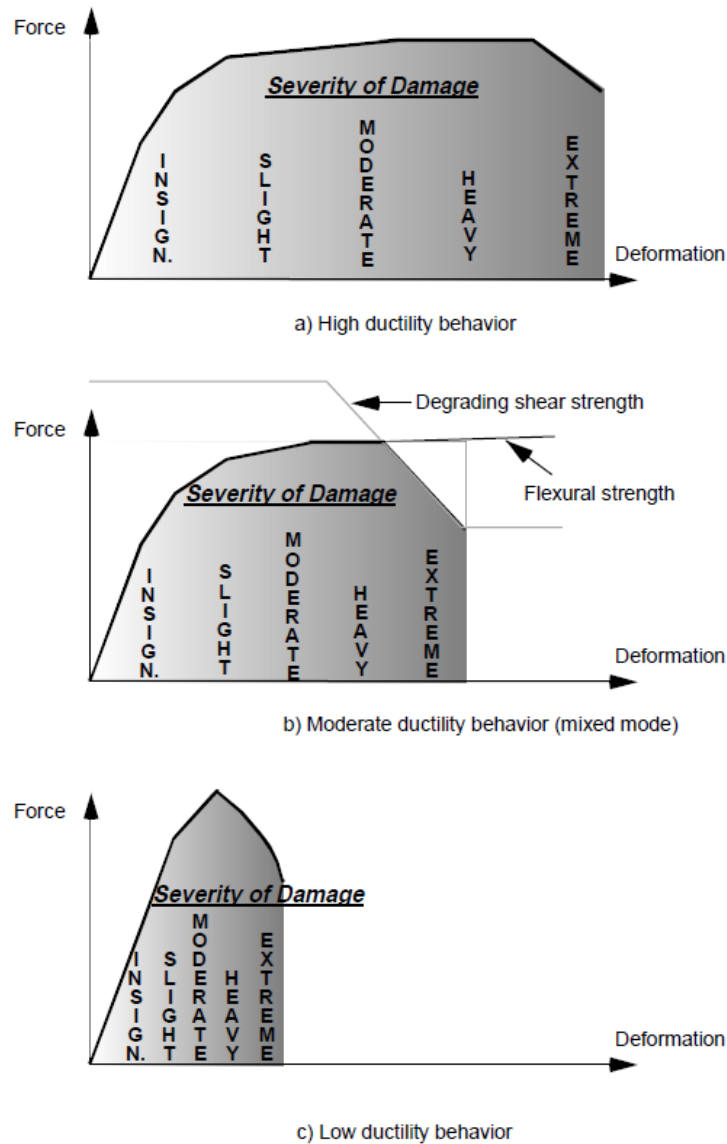


Figure 3. Component force-deformation behavior, ductility, and severity of damage. Source: FEMA 306

Figure 3 presents three typical types of wall behavior depending on the level of ductility. (a) High ductility behavior. This type of behavior is desirable as it allows the structure or component to undergo a large deformation in the post-elastic range and dissipate energy during strong earthquakes, reducing the potential for sudden collapse. Proper reinforcement strength and detailing, appropriate concrete strength, controlled cracking

behavior, and the combination of demand actions (axial, flexural, shearing, torsional) imposed upon it are critical factors in achieving high ductility in reinforced concrete walls and ensuring their reliable performance during seismic events. This ductile response results from a dominant flexural behavior. Plastic hinges occur at the critical regions of wall members where moment demand reaches their flexural strength. Plastic hinges typically occur at the face of a supporting member or foundation for earthquake-induced forces. Existence of lap splices in high moment regions may force plastic hinges to develop or concentrate at the ends of the lap-splice length. A typical flexure failure is shown in Figure 4, and the corresponding load-displacement curve is presented in Figure 5. [8]

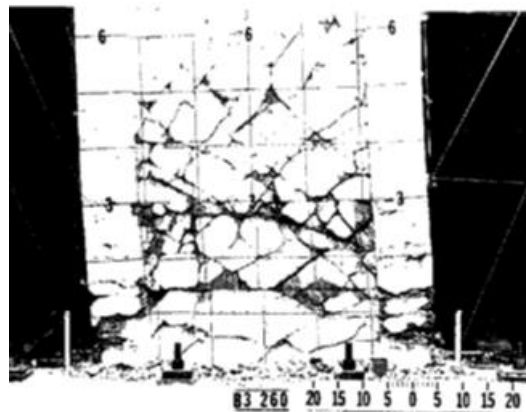


Figure 4. Specimen B3 at the End of the Test. Source: Oesterle et al. (1979)



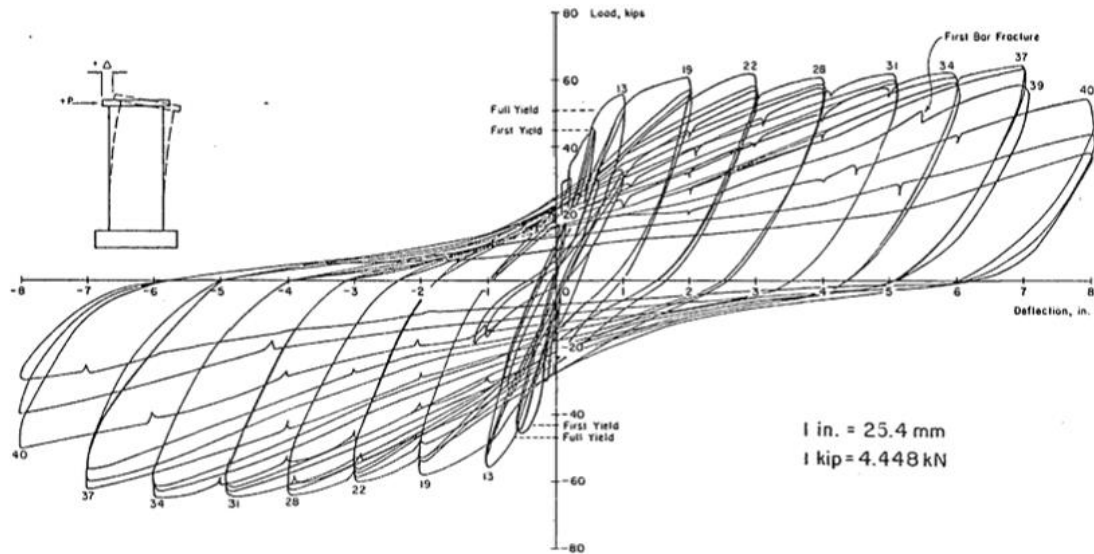


Figure 5. Load-deflection plot for Specimen B3. Source: Oesterle et al. (1979)

(b) Moderate ductility behavior. For reinforced concrete walls with intermediate ductility capacity, the earthquake response is initially driven by flexure. Still, after a certain number of cycles, reaching a certain level of earthquake displacements, a failure mode not related to flexure is triggered. The component's strength has degraded at this point. Figure 3 (b). The possible failure modes are enlisted and explained according to FEMA 306 [9] and FEMA 307 [5]:

- Diagonal tension: occurs in a wall component when the shear strength in diagonal tension initially exceeds the flexural strength, allowing flexural yielding to occur. However, after the cracks open and the concrete in the plastic hinge zone degrades, the shear strength is reduced below the flexural strength, and shear behavior predominates (Figure 6).



Figure 6. Diagonal tension (a) T1-S1, (b) T1-S2, (c) T1-N10-S1. Source: Terzioglu et al. (2018).

- Diagonal Compression (Web crushing): For heavily reinforced walls subject to high shear forces, shear-related compression failures may occur rather than diagonal tension failures. This behavior has been commonly observed in laboratory testing, and it may be prevalent in low-rise walls or when shear reinforcement is sufficient to prevent a diagonal tension failure. Higher axial loads also increase the likelihood of web-crushing behavior. Web crushing generally occurs after some degree of cyclic flexural behavior and degradation. The vulnerability to web crushing can be proportional to the story drift ratio to which the component is subjected. This behavior mode is characterized by diagonal cracking and spalling in the web region of the wall. Localized web crushing can be initiated by the uneven closing of diagonal cracks under cyclic earthquake forces (Figure 7).



Figure 7. Diagonal compression (d) T2-S. Source: Terzioglu et al. (2018).

- Sliding shear: Coupling beams and low-rise walls are particularly vulnerable to failure by sliding shear. Low axial loads and poor construction joint details increase the probability of sliding shear. In this behavior mode, flexural yielding initially governs the response. Flexural cracks at the critical section tend to join up to form a single crack across the section, becoming a potential sliding plane. Under cyclic forces and displacements, this crack opens more widely so that the aggregate interlock and shear friction resistance on the sliding plane degrade. When the sliding shear strength drops below the shear corresponding to the moment strength, lateral sliding offsets begin to occur. For many low-rise walls, lateral strength may be governed by the foundation's strength to resist overturning. Sliding shear behavior is likely to occur only in low-rise walls where the foundations have the capacity to force flexural yielding (Figure 8).

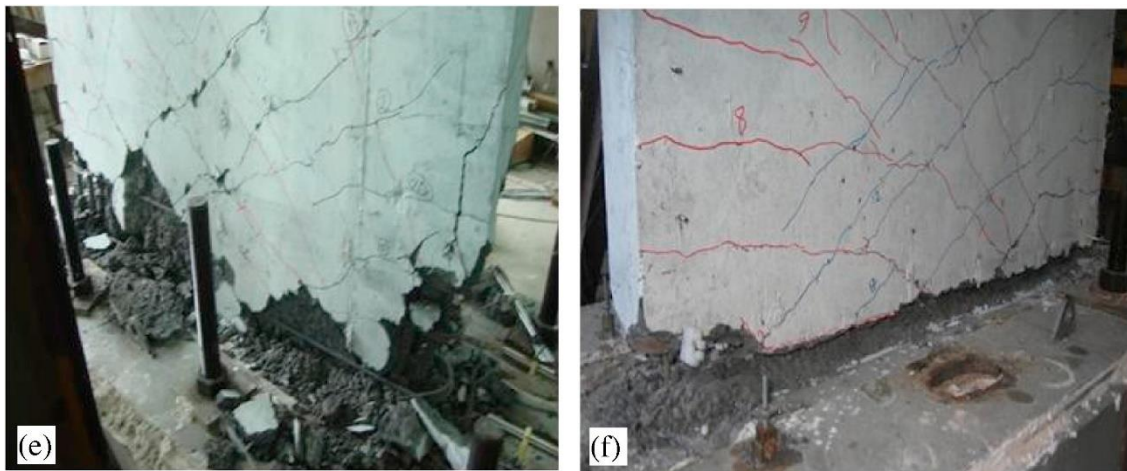


Figure 8. Sliding shear (e) T5-S1, (f) T3-S1. Source: Terzioglu et al. (2018).

- Boundary-zone compression: taller walls with adequate shear strength but inadequate boundary tie reinforcement tend to be vulnerable to this behavior mode. Under inelastic flexural response, the boundary regions of plastic hinge zones may be subjected to high compression strains, which cause spalling of the cover concrete. If sufficient tie reinforcement is not placed around the longitudinal bars in the wall boundaries, the longitudinal bars are prone to buckling. Additionally, in walls where concrete compressive strains exceed 0.004 or 0.005, the concrete in the boundary regions can rapidly lose compressive strength if adequate boundary ties do not confine it. In addition to bar-buckling restraint and confinement, ties around the lap splices of boundary longitudinal bars significantly increase lap-splice strength (Figure 9).

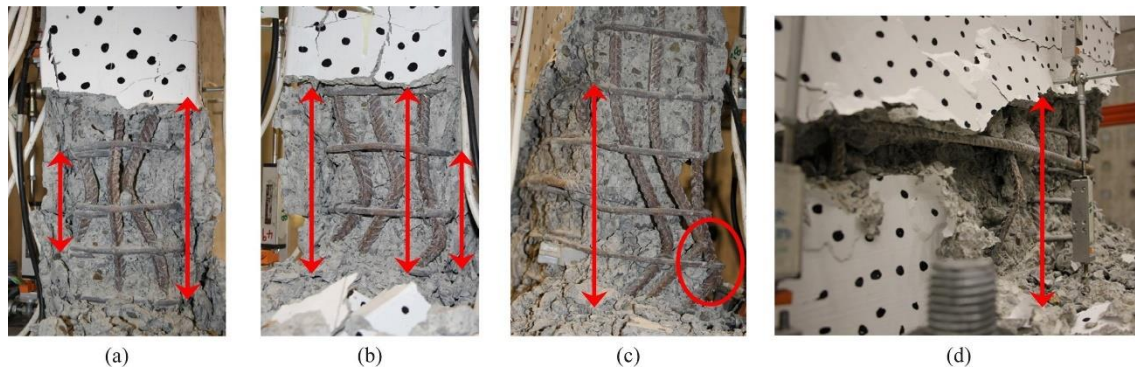


Figure 9. Reinforcement buckling and fracture observed in wall SWD-1. Source: Bar buckling in ductile RC walls with different boundary zone detailing: Experimental investigation. Tripathi et al. (2018).

- Lap-splice slip: Lap splices in the critical plastic hinge regions of walls are commonly encountered in existing buildings. Even when relatively good lap-splice length is provided, lap splices in plastic hinge zones tend to slip when the concrete cover around the lapped bars crushes and/or when they are subjected to large tensile forces. Slipping of lap splices is accompanied by splitting cracks in the concrete, oriented parallel to the spliced reinforcement. The use of tie reinforcement around lap splices, which restrains the opening of the splitting cracks, can prevent or delay the onset of lap-splice slip. Once lap splices slip, the component strength falls below the full moment strength of the section, and the strength is governed by the residual strength of the splices plus the moment capacity due to axial load.
- Out-of-plane wall buckling: Several experimental studies have shown that thin wall sections can experience out-of-plane buckling when subjected to cyclic flexural forces and displacements. For typical wall sections, the buckling occurs only at high ductility levels. Single curtain walls and walls with higher longitudinal reinforcement tend to be more vulnerable to out-of-plane buckling.



Walls with considerable story heights between floors that brace the wall in the out-of-plane direction are more susceptible to buckling. T- or L-shaped wall sections with thin stems may also be more vulnerable. Walls with flanges or other enlarged boundary elements are less susceptible (Figure 10).



*Figure 10. Out-of-plane induced damage in an RC wall after the New Zealand earthquake: Source: Sritharan et al.(2011)*

Low ductility behavior. As shown in Figure 3 (c), some reinforced concrete walls may present low or no ductility during a strong earthquake. For these walls, it is not possible to generate ductile behavior due to deficient design characteristics resulting in brittle failures that occur before flexural yielding occurs. These pre-emptive failures include the following failure modes described before: diagonal tension, diagonal compression, web crushing, sliding shear, boundary zone compression, and lap-splice slip.

---

## 2.2 Damage fragility analysis

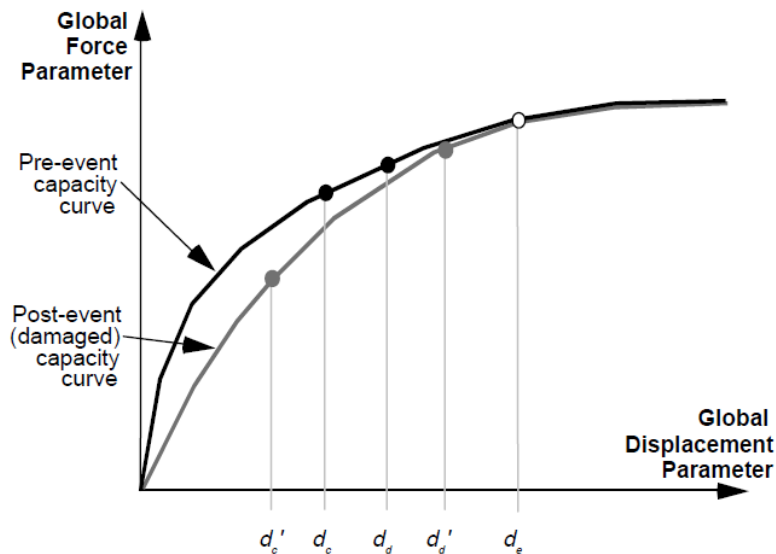
Earthquakes can damage both structural and nonstructural components in buildings. As described in FEMA 273 [10], the performance level is the intended post-earthquake condition of a building; a well-defined point on a scale measuring how much loss is caused by earthquake damage. In addition to casualties, the loss may be in terms of property and operational capability.

The following performance levels are defined in the FEMA 273 document: [10]

- **Immediate Occupancy (IO):** This performance level aims to ensure that the structure remains functional and habitable with limited damage following a seismic event. With all structural components to remain with practically their initial strength and stiffness.
- **Life Safety (LS):** Post-earthquake damage state where the structure has suffered significant damage, but there is still a safety margin against collapse. Structural components are damaged and lose some properties, so structural repairs should be done.
- **Collapse Prevention (CP):** The structure is on the brink of collapsing, partially or entirely. The structure has sustained severe damage, including degradation in the stiffness and strength of the lateral-force-resisting system, significant permanent lateral deformations, and some decrease in vertical-load-carrying capacity. The risk of injury from falling debris is high, and structural repair's technical feasibility may be limited.

To relate performance level to the structure's elements is feasible based on the definition of damage acceptance criteria. This procedure can be assessed either by visual inspection complemented by investigative experiments and structural analysis, and it is possible to generate potential solutions or methods of repair by determining how the structural damage has altered structural characteristics. The damage level can be associated with a capacity curve, which is a graphical representation of the structural capacity of a building or component as a function of the applied demand. It provides valuable information about how the structure or component will behave under different loading levels. The capacity curve is typically obtained through a nonlinear analysis, such as the pushover analysis method. This analysis involves incrementally increasing the lateral forces or displacements applied to the structure until reaching a desired limit or failure condition. As the applied demand increases, the structure's response is tracked, and the corresponding resistance or capacity is determined. The capacity curve is usually plotted with the demand parameter (lateral displacement or base shear) on the x-axis and the capacity parameter (interstory drift or lateral force) on the y-axis. The curve represents the relationship between the demand and capacity, indicating how the structure or component responds to increasing loading levels. The shape of the capacity curve provides insights into the structural behavior. The curve will be linear in the elastic range, indicating a proportional response between demand and capacity. As the demand increases beyond the elastic limit, the curve will deviate from linearity, showing nonlinear behavior and potentially exhibiting strength degradation or stiffness reduction (Figure 11).





- $d_e$  = Estimate of maximum global displacement caused by damaging earthquake
- $d_c$  = Global displacement capacity for pre-event structure for specified performance level
- $d'_c$  = Global displacement capacity for damaged structure for specified performance level
- $d_d$  = Global displacement demand for pre-event structure for specified seismic hazard
- $d'_d$  = Global displacement demand for damaged structure for specified seismic hazard

Figure 11. Displacement Parameters for Damage Evaluation. Source: FEMA 306

Each component's corresponding inelastic force-deformation relationships govern how the structure behaves in undamaged, damaged, and restored states. Each of the building's structural elements will deform in response to a specific global displacement of a system under a given lateral load pattern. The maximum global displacement due to seismic forces ( $d_d$ ) see (Figure 12), could indicate damage to the components due to the inelastic deformations. The maximum global displacement ( $d_c$ ), at which the damage is on the edge of surpassing the limit for the specified performance level, represents a structure's capacity for a given performance level. Restoration of structural elements is necessary to recover or upgrade the performance to its pre-event condition. [11]

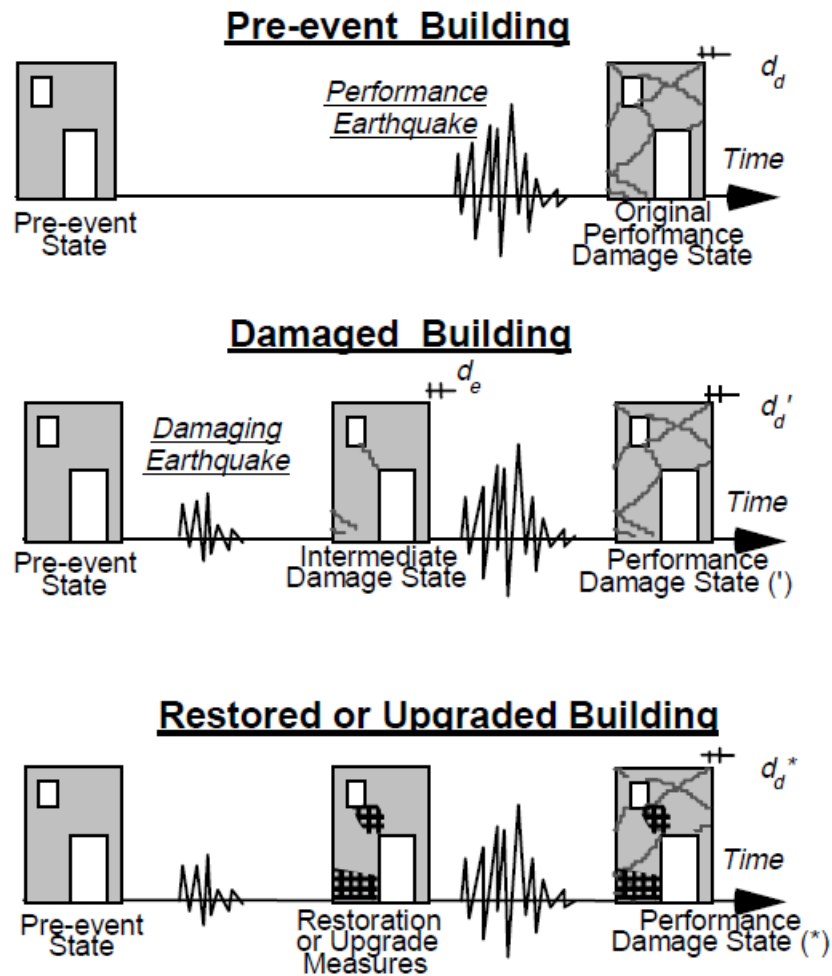


Figure 12. Global displacement demand for undamaged, damaged, and restored/upgraded conditions. Source: FEMA 308

A comparison between a building or component's capacity to withstand lateral movement and the requirement for lateral movement imposed by the performance ground motion is the foundation of performance-based analyses. It is estimating the displacement demand that the damaging earthquake made on a building can provide information about its performance characteristics.

Damage states are a finite set that occurs as a continuum and represents different levels of damage caused to a building or a structural component during a seismic event. These damage states are typically defined based on observable structural performance, such as concrete crack widths, concrete spalling, reinforcement buckling or rupture, and excessive residual deformation. The number and severity of damage states may vary depending on the component or building under consideration. The criteria for each damage state are often set based on engineering judgment, empirical data, or experimental testing. FEMA P-58-V1 (2018) [12] provides a practical way to categorize the extent of damage and assess the performance of structures and components by assigning discrete damage states. This distinct approach streamlines the evaluation process and makes comparing structures or components in similar damage stages easier. The capacity curves can assess the likelihood of each damage state occurring for a given seismic hazard level, which can then be used to build fragility curves or other quantitative seismic performance indicators. [12]

A fragility demand parameter is a metric that indicates the potential occurrence of damage states with reasonable level of uncertainty. Story drift ratio is the most typical demand for structural components as reported in previous research studies, and test results for many structural systems or components are reported in terms of drift. The relative displacement or deformation throughout different levels of the building or element is referred to as the story drift ratio. It accurately indicates possible damageability since it indicates the structure's distortion (deformation) demands.

The probability of achieving or exceeding a certain damage level as a function of a demand parameter such as story drift ratio dissipated hysteretic energy or floor

acceleration is used to build fragility functions for seismic loading. Fragility functions are a significant tool in seismic performance assessment as they allow the probabilistic estimation of component possible damage levels, which can guide risk management and mitigation strategies. They are developed using empirical data, analytical models, or expert judgment and must be thoroughly calibrated and validated based on the specific context and characteristics of the evaluated components. A unique fragility function must be developed for each damage state. These fragility functions can be developed using laboratory testing, earthquake experience data collection, analysis, engineering judgment, or a combination of these methods.

Several laboratory tests on reinforced concrete shear walls were reviewed to collect data for developing fragility curves in which the specific damage and corresponding demand (SDR) were reported. When reviewing previous tests, typical failure modes were identified, along with various types of damage that serve as indicators of the dominant behavior and failure modes. These indicators of damage are:

- Concrete crack width.
- Reinforcement buckling and/or fracture.
- Concrete spalling and crushing (in the cover or wall core).
- Residual displacement.

Specifying the damage's intensity is critical to appropriately define the repair method later. As a result of the increasing damage, the restoration procedure becomes more complex, resulting in a higher cost and time to repair the structure. Table 1 depicts the general relationship between the severity of damage and the expected damage for the structure's components.

Table 1. Component Damage Classification. Source: FEMA 306

Severity of damage	Description
Insignificant	Damage does not significantly affect structural properties despite a minor loss of stiffness. Restoration measures are cosmetic unless the performance objective requires strict limits on nonstructural component damage in future events.
Slight	Damage has a negligible effect on structural properties. Relatively minor structural restoration measures are required for most components and behavior modes.
Moderate	Damage has an intermediate effect on structural properties. The scope of restoration measures depends on the component type and behavior mode. Measures may be relatively major in some cases.
Heavy	Damage has a major effect on structural properties. The scope of restoration measures is generally extensive. Replacement or enhancement of some components may be required.
Extreme	Damage has reduced structural performance to unreliable levels. The scope of restoration measures generally requires the replacement or enhancement of components.

Once the severity of the damage has been determined, it is possible to estimate the proper repair action to be made; this can be to accept, restore or upgrade the structural element by how it was performed after the seismic event. These potential structural component repairs are referred to as performance restoration measures and must be done so the structural component meets the same or close performance as the undamaged structure;

the economic loss may be calculated as the cost of the restoration process. The categories of repair after the observed damage are: [11]

- **Cosmetic Repair:** These repairs restore nonstructural properties such as visual appearance or weather protection.
- **Structural Repair:** Repair component damage to restore structural properties.
- **Structural Enhancement:** These repairs include either further additions or the removal and replacement of existing damaged components. Instead of restoring damaged components, the goal is to replace their structural characteristics.

Table 2, present the repair types for each repair structural category and material according to FEMA 308 (1998) [11].

Table 2. Summary of repair procedures. Source: FEMA 308

Repair Category	Material			Repair ID	Repair Type
	Reinf. Concrete	Reinf. Masonry	URM		
Cosmetic Repair	√	√	√	CR 1	Surface coating
			√	CR 2	Repointing
	√	√*		CR 3	Crack injection with epoxy
Structural Repair	√	√*		SR 1	Crack injection with epoxy
	√	√	√	SR 2	Crack injection with grout
	√	√		SR 3	Spall repair
	√			SR 4	Rebar replacement
	√	√	√	SR 5	Wall replacement
Structural Enhancement	√	√	√	SE 1	Concrete overlay
	√	√	√	SE 2	Composite Fibers
	√			SE 3	Crack Stitching

Notes: Repairs for concrete walls can also be used for concrete frames in infilled frame systems.

Repairs for steel frames of infill systems are described in the component repair guides.

\* Epoxy injection not recommended for partially-grouted reinforced masonry.

---

## 3 Methodology for developing fragility functions

### 3.1 Overview

The fragility functions developed in the present study are intended to be used with the FEMA P-58 framework for seismic assessment of existing buildings [9]. This framework follows a probabilistic approach accounting for the uncertainties associated with the seismic hazard, ground motion, and structural response. The assessment process for a reinforced concrete wall building would involve several steps, including modeling the wall system's behavior, selecting and scaling ground motions, performing structural analysis, and developing fragility curves. The fragility curves related the structural response to the conditional probability of exceeding a specific damage state.

Analyzing the structural response involves setting a mathematical model of the wall system using finite element analysis or other numerical methods; the model accounts for the physical properties of the wall, including its size, shape, and material properties. It also involves finding ground motions to match the seismic hazard levels identified for the site; including selection of a set of ground motion records from a database of recorded earthquakes and scaling them to fit the seismic hazard levels. The scaling accounts for the site-specific characteristics of the wall, such as soil conditions and the wall's period. Then performing structural analysis to determine the wall's response to the selected ground motions. Uncertainties associated with seismic hazards, ground motion, and structural response must be considered in the analysis. Finally, fragility curves are needed to relate the probability of damage or collapse of the wall to the intensity of the ground motion—fitting statistical models to develop fragility curves to the structural analysis results.

Fragility functions are developed in this study for reinforced concrete walls in low-rise housing following the actual demand method presented in the FEMA P-58 methodology. In order to develop these functions, damage states are defined, a database of experimental data is compiled, and fragility parameters are derived on the analysis of experimental data.

### **3.2 Definition of Damage States**

A systematic methodology is adopted to present the damage states for reinforced concrete shear walls, including detailed observation, analysis, and categorization of the observed damage in laboratory tests by Carrillo and Alcocer [2] and Hidalgo [3]. The following steps outline the approach used to characterize the three damage states proposed for reinforced concrete shear walls with a shear-dominated behavior: slight, moderate, and severe.

The first step in the methodology is to collect data from experimental tests, field investigations, and literature reviews; for this, an essential database with shear walls is presented by Gulec [13]. This database provides valuable insights into the behavior of reinforced concrete shear walls under seismic loads and serves as a basis for understanding the damage states. Nevertheless, this database was not directly used to develop fragility data in the present study, as many of the wall tests did not represent low-rise wall construction in Latin America.



A thorough observation and documentation process is conducted. This involves visually inspecting and documenting the condition of shear walls subjected to seismic events or laboratory tests. Special attention is given to cracks, deformations, and other visible signs of damage. Digital photographs and sketches are captured to provide visual evidence of the observed damage, as shown in Figure 13 and Figure 14.



*Figure 13. Model MCN100D before the test. Source: Carrillo (2010)*

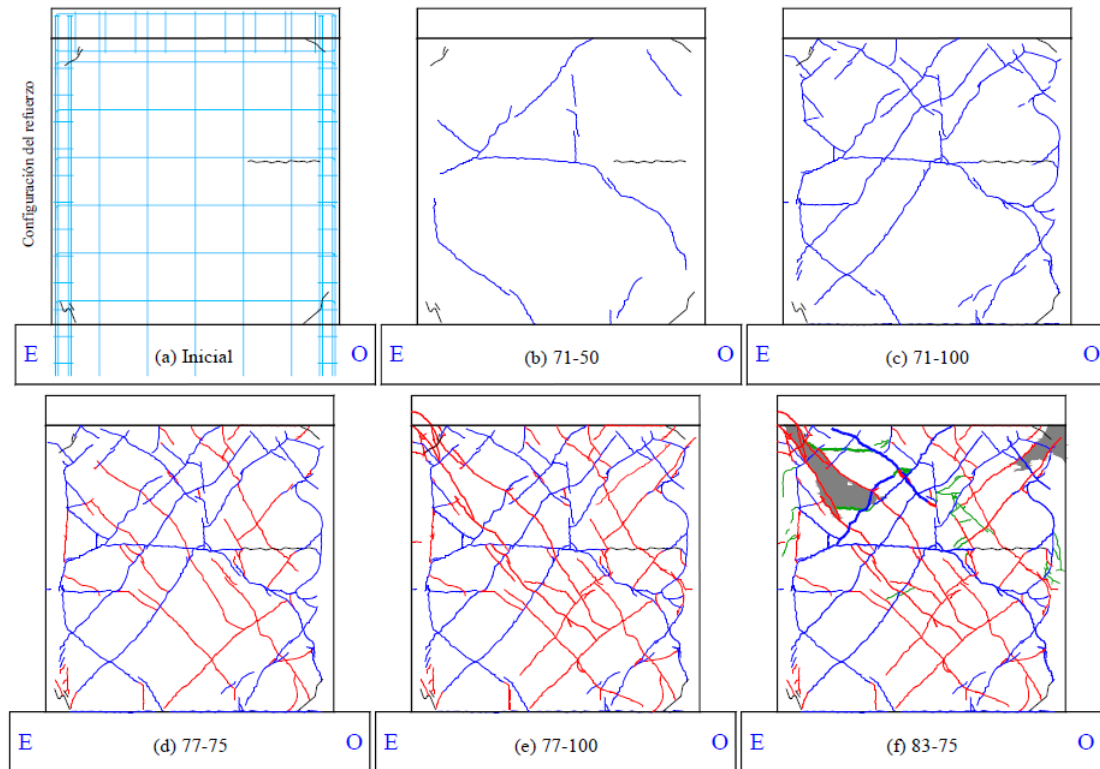


Figure 14. Cracking evolution of Model MCN100D. Source: Carrillo (2010)

Based on the collected data and observations, the damage is classified into three distinct severity of damage: slight, moderate, and severe. Each damage state is characterized by specific criteria and indicators, which allow for consistent and reliable classification.

For the "Slight" damage state, the key indicator is the presence of diagonal cracking within the shear wall. These cracks are typically narrow and superficial and do not significantly affect the overall structural performance.

The "Moderate" damage state, known as the Life Safety state, is characterized by more prominent cracking and deformation. The cracks may be wider and more extensive,

impacting the stability of the structure. However, the shear wall still retains sufficient residual strength to prevent complete collapse, ensuring the safety of occupants.

In the "Severe" damage state, the shear wall has reached its peak shear strength capacity. Extensive cracking, large deformations, and potential failure of critical components are observed. At this stage, the shear wall is unable to resist further seismic forces, posing a significant risk to the structure's integrity.

Following the "Component Damage Classification Guide" from FEMA 306 and the behavior modes reported on the laboratory test by Carrillo & Alcocer, Diagonal Tension, Diagonal Compression, and a mixed Diagonal Tension and Compression. Table 3 and Table 4.

- RC1B – Behavior mode: Flexural/Diagonal Tension: Typically happens in walls with low-to-moderate horizontal reinforcement and heavy vertical (flexural) reinforcement. It is most common in walls with intermediate aspect ratios,  $\frac{M}{V \times l_w} > 2$ , but it can occur in walls with a wide range of aspect ratios depending on the reinforcement. Shear cracking can occur at low ductility levels. One or more wide shear cracks begin to appear at increased levels of damage. Shear strength predicted for low ductility conditions exceeds flexural capacity. However, shear strength calculated for high ductility conditions is less than flexural capacity.
- RC1C – Behavior mode: Flexure/Web Crushing (Diagonal Compression): Typically happens in walls with adequate horizontal reinforcement in addition to significant vertical (flexural) reinforcement. Low-rise walls, walls with higher axial loads, and heavy boundary elements may be more susceptible. Extensive

---

diagonal cracking and spalling of web areas begin to develop at greater levels of damage. Web crushing strength, calculated for high levels of story drift ductility, is less than flexural strength. Conditions of high ductility are less than the flexural capacity.

For the "Slight" damage state, the key indicator is the presence of diagonal cracking within the shear wall. These cracks are typically narrow and superficial and do not significantly affect the overall structural performance.

The "Moderate" damage state, known as the Life Safety state, is characterized by more prominent cracking and deformation. The cracks may be wider and more extensive, impacting the stability of the structure. However, the shear wall still retains sufficient residual strength to prevent complete collapse, ensuring the safety of occupants.

In the "Severe" damage state, the shear wall has reached its peak shear strength capacity. Extensive cracking, large deformations, and potential failure of critical components are observed. At this stage, the shear wall is unable to resist further seismic forces, posing a significant risk to the structure's integrity.

Table 3. RC1B Component Damage Classification Guide. Source: FEMA 306

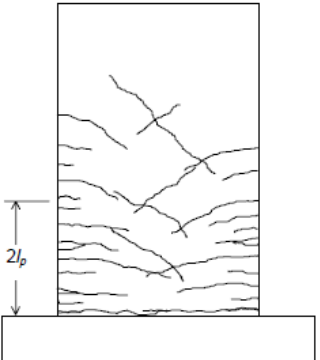
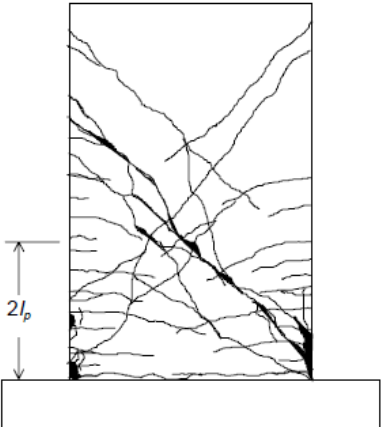
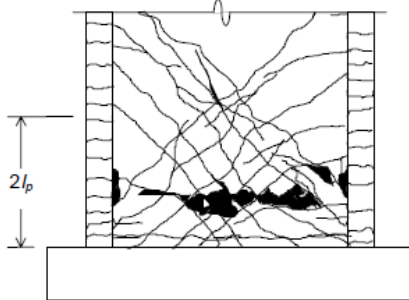
RC1B		COMPONENT DAMAGE CLASSIFICATION GUIDE	System: Reinforced Concrete
			Component Type: Isolated Wall or Stronger Pier
			Behavior Mode: Flexure/Diagonal Tension
Severity	Description of Damage	Performance Restoration Measures	
Insignificant  $\lambda_K = 0.8$ $\lambda_Q = 1.0$ $\lambda_D = 1.0$	<p><i>Criteria:</i></p> <ul style="list-style-type: none"> <li>• Shear crack widths do not exceed 1/16 in., <u>and</u></li> <li>• Flexural crack widths do not exceed 3/16 in., <u>and</u></li> <li>• No significant spalling or vertical cracking.</li> </ul> <p><i>Typical Appearance:</i></p>  <p style="text-align: right;"><i>Note:</i> <math>l_p</math> is length of plastic hinge. See Section 5.3.3</p>	(Repairs may be necessary for restoration of nonstructural characteristics.)	
Slight	Not Used		
Moderate  $\lambda_K = 0.5$ $\lambda_Q = 0.8$ $\lambda_D = 0.9$	<p><i>Criteria:</i></p> <ul style="list-style-type: none"> <li>• Shear crack widths do not exceed 1/8 in., <u>and</u></li> <li>• Flexural crack widths do not exceed 1/4 in., <u>and</u></li> <li>• Shear cracks exceed 1/16 in., <u>or</u> limited spalling (or incipient spalling as identified by sounding) occurs at web or toe regions, <u>and</u></li> <li>• No buckled or fractured reinforcement, <u>and</u></li> <li>• No significant residual displacement.</li> </ul> <p><i>Typical Appearance:</i> Similar to insignificant damage except wider cracks, possible spalling, and typically more extensive cracking.</p>	<ul style="list-style-type: none"> <li>• Remove and patch spalled and loose concrete. Inject cracks.</li> </ul> $\lambda_K^* = 0.8$ $\lambda_Q^* = 1.0$ $\lambda_D^* = 1.0$	
Heavy  $\lambda_K = 0.2$ $\lambda_Q = 0.3$ $\lambda_D = 0.7$	<p><i>Criteria:</i></p> <ul style="list-style-type: none"> <li>• Shear crack widths may exceed 1/8 in., but do not exceed 3/8 in. Higher cracking width is concentrated at one or more cracks.</li> </ul> <p><i>Typical Appearance:</i></p>  <p style="text-align: right;"><i>Note:</i> <math>l_p</math> is length of plastic hinge. See Section 5.3.3</p>	<ul style="list-style-type: none"> <li>• Replacement or enhancement is required for full restoration of seismic performance.</li> <li>• For <u>partial</u> restoration of performance, inject cracks</li> </ul> $\lambda_K^* = 0.5$ $\lambda_Q^* = 0.8$ $\lambda_D^* = 0.8$	
Extreme	<p><i>Criteria:</i></p> <ul style="list-style-type: none"> <li>• Reinforcement has fractured.</li> </ul> <p><i>Typical Indications</i></p> <ul style="list-style-type: none"> <li>• Wide shear cracking typically concentrated in a single crack.</li> </ul>	<ul style="list-style-type: none"> <li>• Replacement or enhancement required.</li> </ul>	

Table 4. RC1C Component Damage Classification Guide. Source: FEMA 306

RC1C		COMPONENT DAMAGE CLASSIFICATION GUIDE	System: Reinforced Concrete
			Component Type: Isolated Wall or Stronger Pier
			Behavior Mode: Flexure/Web Crushing
Severity	Description of Damage		Performance Restoration Measures
Insignificant	$\mu_{\Delta} \leq 3$	See RC1B	See RC1B
Slight	Not Used		
Moderate $\lambda_K = 0.5$ $\lambda_Q = 0.8$ $\lambda_D = 0.9$	<p><i>Criteria:</i></p> <ul style="list-style-type: none"> <li>• Shear crack widths do not exceed 1/8 in., <u>and</u></li> <li>• Flexural crack widths do not exceed 1/4 in., <u>and</u></li> <li>• Limited spalling (or incipient spalling as identified by sounding) occurs at web or toe regions, <u>or</u> shear cracks exceed 1/16 in., <u>and</u></li> <li>• No buckled or fractured reinforcement, <u>and</u></li> <li>• No significant residual displacement.</li> </ul>		<ul style="list-style-type: none"> <li>• Remove and patch spalled and loose concrete. Inject cracks.</li> </ul> <p style="text-align: center;"><math>\lambda_K^* = 0.8</math> <math>\lambda_Q^* = 1.0</math> <math>\lambda_D^* = 1.0</math></p>
Heavy  $\lambda_K = 0.2$ $\lambda_Q = 0.3$ $\lambda_D = 0.7$	<p><i>Criteria:</i></p> <ul style="list-style-type: none"> <li>• Significant spalling of concrete in web, <u>and</u></li> <li>• No fractured reinforcement.</li> </ul> <p><i>Typical Appearance:</i></p>  <p style="text-align: center;">Note: <math>l_p</math> is length of plastic hinge. See Section 5.3.3</p>		<ul style="list-style-type: none"> <li>• Remove and patch all spalled and loose concrete. Inject cracks.</li> </ul> <p style="text-align: center;"><math>\lambda_K^* = 0.8</math> <math>\lambda_Q^* = 1.0</math> <math>\lambda_D^* = 1.0</math></p>
Extreme	<i>Criteria:</i>	<ul style="list-style-type: none"> <li>• Heavy spalling and voids in web concrete, <u>or</u> significant residual displacement.</li> </ul>	<ul style="list-style-type: none"> <li>• Replacement or enhancement required.</li> </ul>

Each damage state is thoroughly documented, including descriptions, criteria, and visual evidence in tests Table 5. The proposal made in this table allows for a clear and concise presentation of the damage states to aid in the understanding and assessment of the shear wall's seismic performance.

Table 5. Damage States - Seismic fragility functions for reinforced concrete walls in low-rise housing.

<i>Damage States – Seismic fragility functions for reinforced concrete walls in low-rise housing</i>				
ID	Damage State	Description of the damage	Identification criteria to calibrate functions	***Method of Repair
DS1	Slight	Occurrence of the first cracking inclined and distributed over the web of the wall	Shear forces is equal to cracking shear force: $V_{cr} = \alpha_c \lambda \sqrt{f'_c} A_w$ <b>OR</b> The first inclined web crack was observed, caused by diagonal tension forces.[2]	Cosmetic Repair: These repairs restore nonstructural properties such as visual appearance or weather protection.
DS2	Moderate	*Extension of web-inclined cracks to the wall edges without penetration into the boundary elements	Crack width: $- w_{max} < 0.15 \text{ mm}$ <b>AND/OR</b> $I_{crack} < 0.04\%$ for concrete shear walls with welded-wire mesh reinforcement	Epoxy Repair (structural Repair)

			$- w_{max} < 0.40 \text{ mm}$ AND/OR $I_{crack} < 0.10\%$ for concrete shear walls with deformed bars	
DS3	Severe	**Noticeable web diagonal cracking and/or yielding of some web steel bars/wires. Moderate web crushing of concrete and damage around openings.	The peak shear strength $(V_{max})$ is achieved.	Wall Replacement/ Rebar replacement (structural Enhancement)
<ul style="list-style-type: none"> <li>• *-No Data Available</li> <li>• **- It is assumed by a visual report from the test made by Hidalgo (2002).</li> <li>• ***- Table 2. Summary of repair procedures. Source: FEMA 308</li> <li>• <math>V_{max}</math> – is calculated as ACI-318: <math>V_n = V_c + V_s \leq 0.83\lambda\sqrt{f'_c}t_w(0.8l_w)(MPa)</math></li> <li>• <math>V_{cr}</math> – is calculated as ACI-318: <math>V_{cr} = \alpha_c\lambda\sqrt{f'_c}A_w</math></li> <li>• <math>w_{max}</math>: Width of residual crack</li> <li>• <math>I_{crack} = \frac{\Sigma (l_{crack} \times w_{crack})}{A_{facade}}</math>; Where <math>l_{crack}</math>, <math>w_{crack}</math> are length and width of the maximum residual crack. And <math>A_{fachada}</math> is the total area of the original façade.</li> </ul>				

In the experimental program of Hidalgo [3], a description of the damage is not given once the peak shear strength is attained. Therefore, from figures (Figure 15) and (Figure 16) a description of damage such as that proposed by Carrillo and Alcocer [2] is assumed.



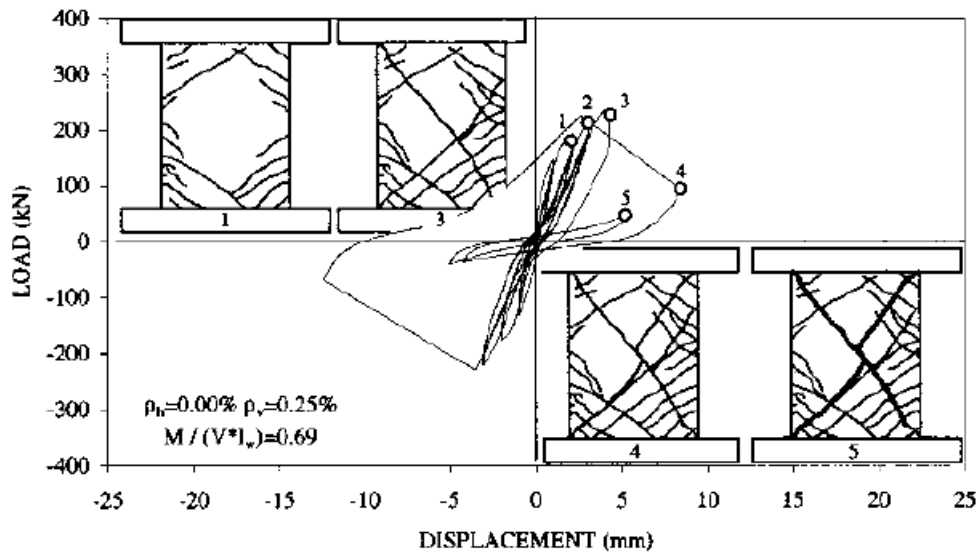


Figure 15. Hysteresis curve for specimen 24. Source: Hidalgo

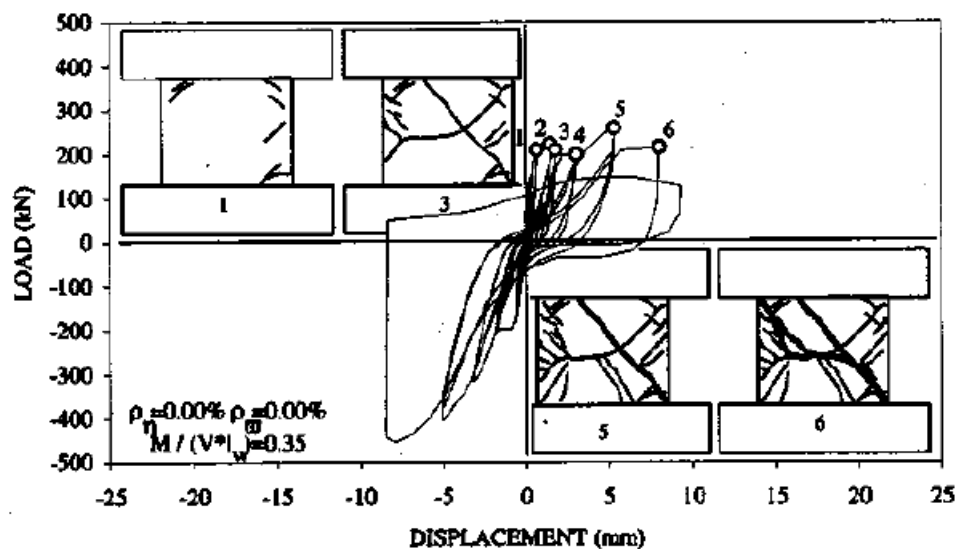


Figure 16. Hysteresis curve for specimen 30. Source: Hidalgo

The collected data and documented damage states are analyzed to identify patterns, trends, and relationships. Statistical analysis is employed to quantify the frequency and severity of each damage state. This analysis helps to understand the behavior of reinforced concrete shear walls and provides valuable information for design, retrofitting, and maintenance purposes. The resulting information enhances our understanding of the

performance of these structural elements under seismic loading conditions. It assists engineers and designers in making informed decisions to ensure the safety and resilience of structures.

### 3.2.1 Data Collection

Several experimental programs were reviewed to gather information on reinforced concrete squat walls to define damage states for developing fragility functions. Gulec and Whitakker's [13]squat-wall database was analyzed to identify potential experimental programs with relevant information for the construction of a database for this investigation. By accessing and analyzing these reports, pertinent data such as: wall's geometry, concrete compressive strength, moment-to-shear ratio, and web steel ratio, so pertinent data was extracted to develop fragility function and damage state assessment. A database specifically representing low-rise construction in Latin America was assembled, enlisting the characteristics of walls and their respective test results. This database includes test data on rectangular reinforced concrete walls from studies by Hidalgo (2002) and Carrillo and Alcocer (2012). These reports include relevant information such as experimental test results, structural performance evaluations, failure modes, material properties, and observed damage patterns in shear walls subjected to seismic loading. From the reports, we identify key parameters and variables essential for understanding the type of designs and developing damage fragility functions. These include the following geometric and material parameters:

- Height-to-length ratio  $\left(\frac{M}{vl_w}\right)$ : Walls with a ratio of less than 2.0 were sought to evaluate shear behavior. (Figure 17)
- Concrete compressive strength  $(f'_c)$  (Figure 18)

- 
- Concrete type: Normalweight, lightweight, and self-consolidating.
  - Web reinforcement ( $f_y$ ): was placed in a single layer at wall mid-thickness.
  - Web steel ratio ( $\rho$ ): The minimum web steel ratio ( $\rho_{min}$ ) was prescribed by the American Concrete Institute's Building Code (ACI-318 2011). (Figure 19)
  - Boundary elements: To assess wall lateral shear strength, longitudinal boundary reinforcement was purposely designed to prevent flexural failure before achieving a shear failure.

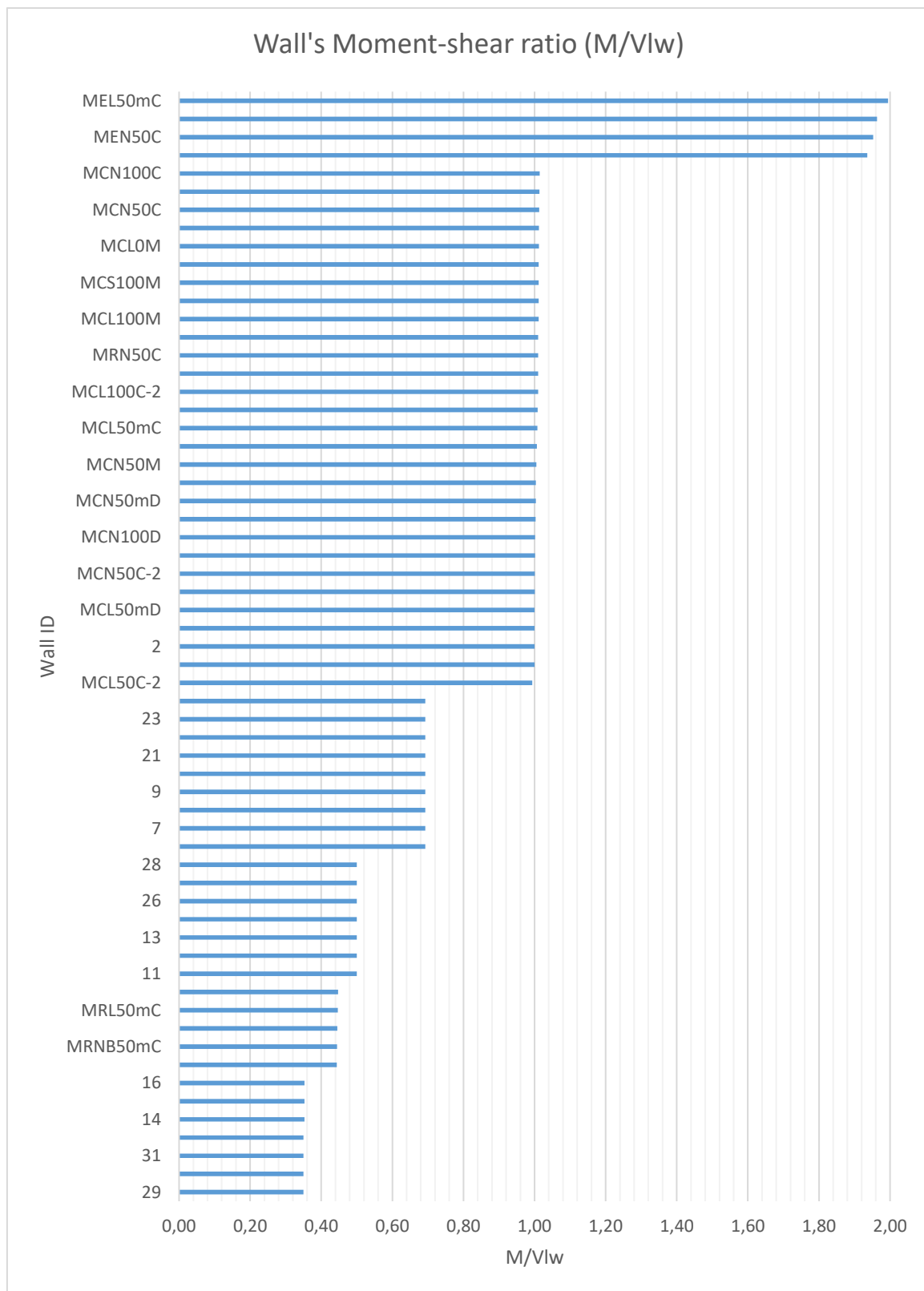


Figure 17. Wall's Height-to-length ratio

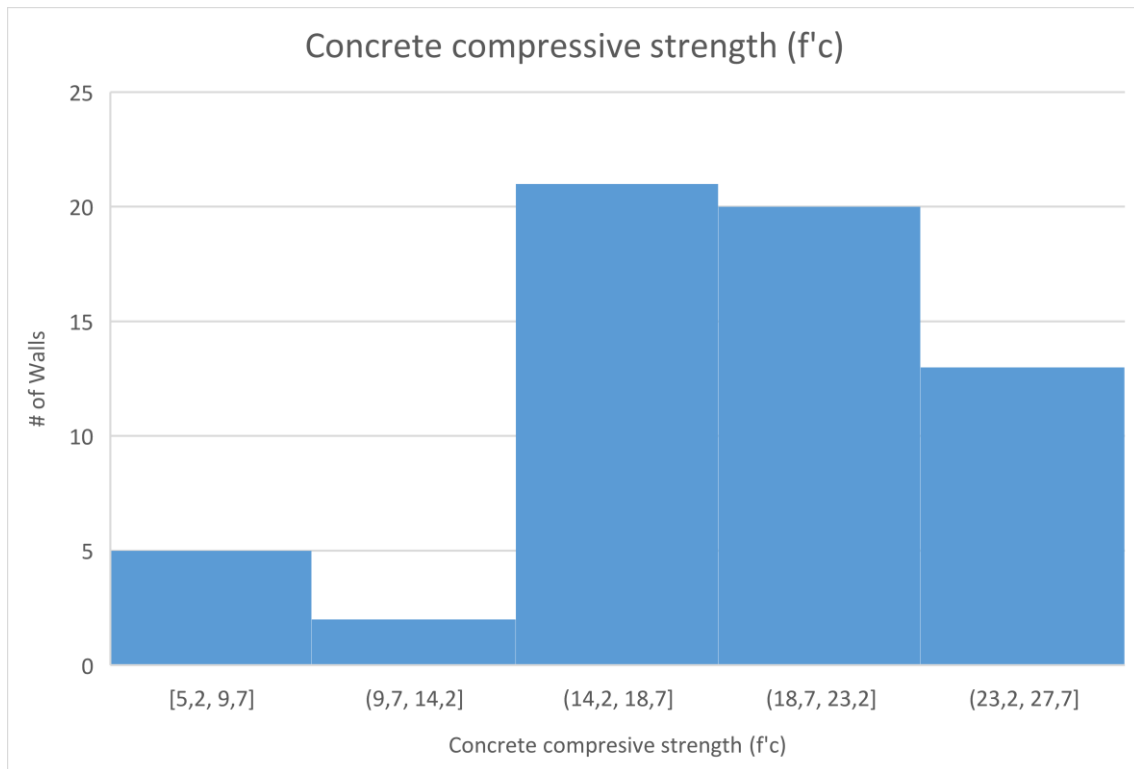


Figure 18. Concrete compressive strength of the walls

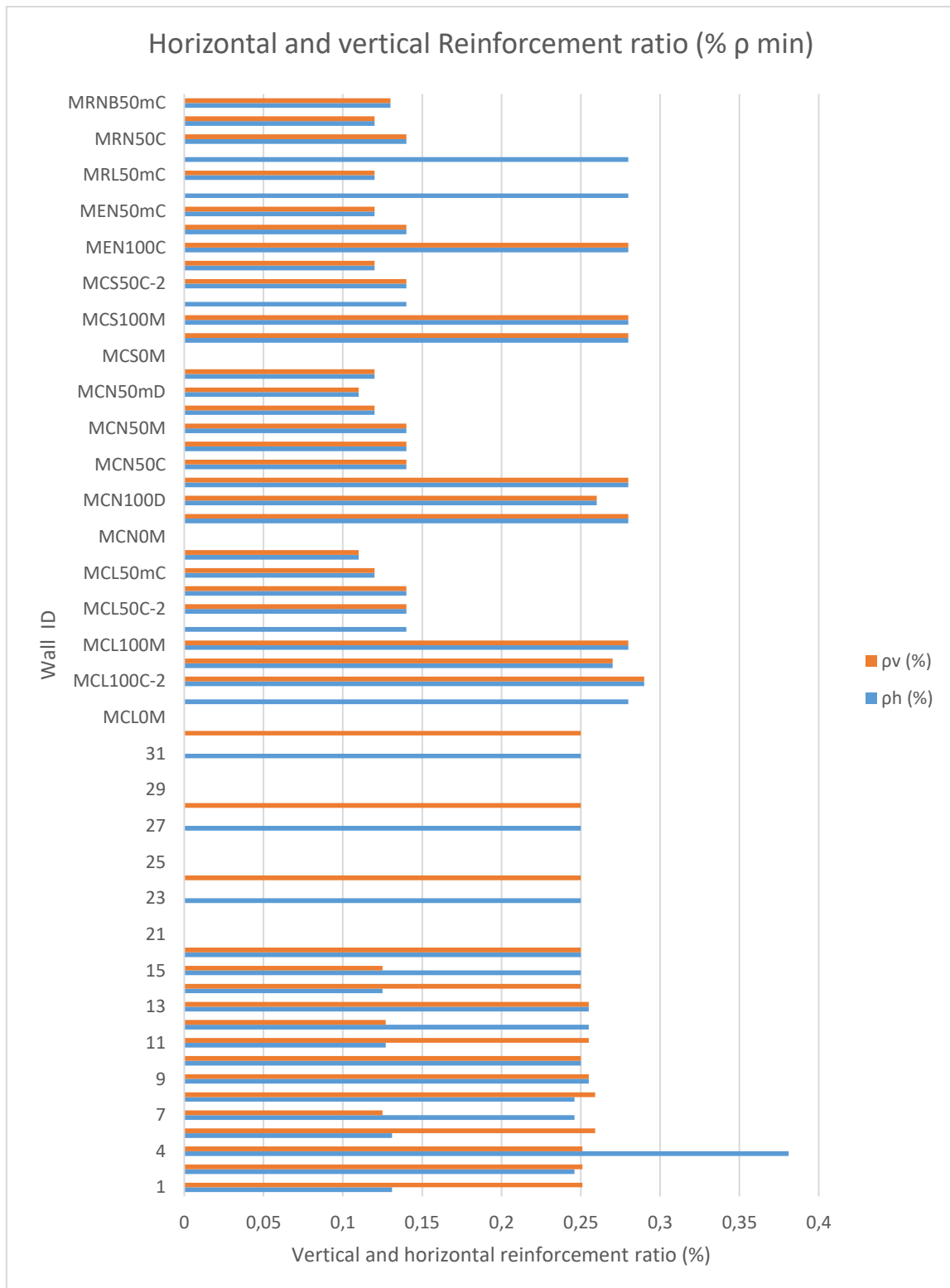


Figure 19. Horizontal and vertical (% of  $\rho$  min)

Collecting and organizing these data relationships can be established between demand and damage. A total of 61 reinforced concrete shear walls tested by Carrillo & Alcocer, and Hidalgo were comprised in this study to develop the fragility functions.

### 3.2.1.1 Tests by Carrillo & Alcocer

The response of 39 reinforced concrete shear walls with different height-to-length ratios was studied by means of quasi-static tests (monotonic and reversed-cyclic) and dynamic loading. Characteristics of the walls are enlisted:

- Height-to-length ratio  $\left(\frac{M}{Vl_w}\right)$ : Varying between 0.5 and 2.0.
- Reinforced concrete shear walls with a rectangular cross-section. Figure 20
- Concrete compressive strength ( $f'_c$ ): Varying between 15 MPa and 25 MPa. Figure 21.
- Concrete type: Normalweight, lightweight, and self-consolidating.
- Axial compressive stress ( $\sigma_v$ ): An axial compressive stress of 0.25 MPa was applied at the top of the walls and was kept constant during the testing. This value corresponded to an average axial stress in the first-floor walls of a two-story prototype house is less than  $0.03 (f'_c)$ .
- Web reinforcement ( $f_y$ ): Web reinforcement with welded-wire mesh or deformed bars were used. Placed in a single layer at wall mid-thickness and same horizontal and vertical reinforcement ratios. Figure 22
- Web steel ratio  $\rho$  : The minimum web steel ratio ( $\rho_{min}$ ) was prescribed by the American Concrete Institute's Building Code (**ACI-318 2011**).

- Boundary elements: To assess wall lateral shear strength, longitudinal boundary reinforcement was purposely designed to prevent flexural failure before achieving a shear failure. The thickness of the boundary elements is equal to the thickness ( $t_w$ ) of the wall web.

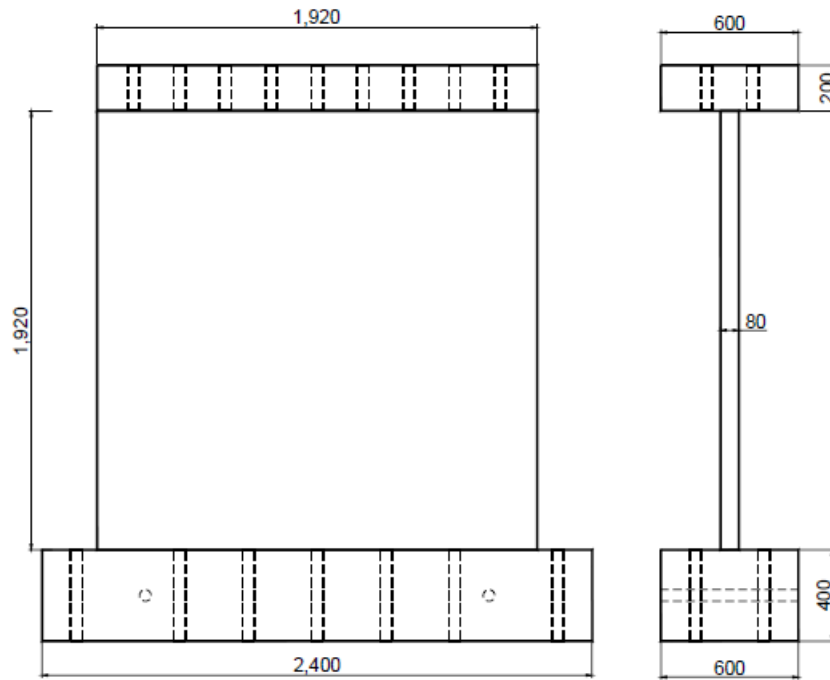


Figure 20. Geometry of square cross-section walls. Source: Carrillo (2010)

Type	Normal weight, N	Lightweight, L	Self-consolidating, S
Compressive strength, $f_c$ , MPa	16.0–24.7	10.8–26.0	22.0–27.1
Elastic modulus, $E_c$ , MPa	8430–14750	6700–10790	8900–11780
Tensile splitting strength, $f_t$ , MPa	1.55–2.20	1.14–1.76	1.58–1.98
Flexural strength, $f_r$ , MPa	2.32–3.75	1.43–3.29	2.27–2.48
Specific dry weight, $\gamma$ , kN/m <sup>3</sup>	18.8–20.3	15.2–18.3	18.9

Figure 21. Measured mechanical properties of concrete. Source: Backbone Model for Performance-Based Design of RC Walls for Low-Rise Housing



Location in the wall	Boundary: deformed bar	Web: deformed bar, D	Web: welded-wire, W
Type	Mild	Mild	Cold-drawn
Yield strength, $f_y$ , MPa	411–456	435–447	605–630
Ultimate strength, $f_{su}$ , MPa	656–721	659–672	687–700
Elongation, %	9.1–16.0	10.1–11.0	1.4–1.9

Figure 22. Measured mechanical properties of steel reinforcement. Source: Backbone Model for Performance-Based Design of RC Walls for Low-Rise Housing

Table 6. Explains the mechanical and geometrical properties of wall identification.

Table 6. Wall Identification

<i>Wall Identification - Backbone Model for Performance-Based Seismic Design of RC Walls for Low-Rise Housing</i>										
<b>M</b>	<b>C</b>		<b>N</b>		<b>50</b>		<b>m</b>		<b>D</b>	
"Muro"	Height-to-length ratio		Concrete type		Web steel reinforcement ratio		Type of web reinforcement		Type of testing procedure	
	$\left(\frac{M}{Vl_w}\right)$		-		% of ( $\rho_{min}$ ) by ACI-2011		-		-	
	0.5	<b>R</b>	Normal weight	<b>N</b>	100%	100	-	Deformed bars	<b>D</b>	Dynamic
	1.0	<b>C</b>	Lightweight	<b>L</b>	50%	50	<b>m</b>	Welded-wire mesh	<b>M</b>	Monotonic
	2.0	<b>E</b>	Self-consolidating	<b>S</b>	0%	0	-	-	<b>C</b>	Cyclic
Walls with openings	<b>V</b>	-	-	-	-	-	-	-	-	

The geometrical and mechanical properties of each specimen are presented in Table 7.

Table 7. Wall's geometrical and mechanical properties. Carrillo and Alcocer

Wall ID	Type of testing	Type of concrete	$f_c$ (MPa)	Web reinforcement	$f_y$ (MPa)	$\rho_v$ (%) = $\rho_h$ (%)	tw (mm)	hw (mm)	lw (mm)	M/Vlw
MCL0M	QSM	L	16.3	-	-	0	101	2428	2398	1.01
MCL100C	QSRC	L	10.8	D	447	0.28	101	2424	2399	1.01
MCL100C-2	QSRC	L	5.2	D	447	0.29	98	2432	2407	1.01
MCL100D	DST	L	21	D	435	0.27	82	1918	1912	1.00
MCL100M	QSM	L	16.3	D	447	0.28	101	2425	2398	1.01
MCL50C*	QSRC	L	10.8	D	447	0.14	101	2426	2398	1.01
MCL50C-2	QSRC	L	26	D	447	0.14	100	2426	2441	0.99
MCL50M	QSM	L	16.3	D	447	0.14	102	2427	2397	1.01
MCL50mC	QSRC	L	26	W	605	0.12	100	2423	2403	1.01
MCL50mD	DST	L	21	W	630	0.11	82	1917	1917	1.00
MCN0M	QSM	N	18.8	-	-	0	101	2412	2403	1.00
MCN100C	QSRC	N	17.5	D	447	0.28	101	2432	2397	1.01
MCN100D	DST	N	24.7	D	435	0.26	84	1924	1921	1.00
MCN100M	QSM	N	18.8	D	447	0.28	101	2417	2402	1.01
MCN50C	QSRC	N	17.5	D	447	0.14	102	2431	2399	1.01
MCN50C-2	QSRC	N	20	D	447	0.14	100	2400	2398	1.00
MCN50M	QSM	N	18.8	D	447	0.14	102	2415	2402	1.01
MCN50mC	QSRC	N	20	W	605	0.12	103	2396	5398	0.44
MCN50mD	DST	N	24.7	W	630	0.11	83	1923	1916	1.00
MCNB50mC	QSRC	N	8.9	W	605	0.12	102	2404	2401	1.00
MCS0M	QSM	S	19.4	-	-	0	102	2425	2398	1.01
MCS100C	QSRC	S	22	D	447	0.28	103	2426	2401	1.01
MCS100M	QSM	S	19.4	D	447	0.28	102	2424	2397	1.01
MCS50C*	QSRC	S	22	D	447	0.14	102	2424	2403	1.01
MCS50C-2	QSRC	S	27.1	D	447	0.14	104	2404	2402	1.00
MEL50mC	QSRC	L	26	W	605	0.12	100	2435	1221	1.99
MEN100C	QSRC	N	16.2	D	447	0.28	100	2435	1240	1.96
MEN50C	QSRC	N	16.2	D	447	0.14	100	2421	1240	1.95
MEN50mC	QSRC	N	20	W	605	0.12	101	2399	1239	1.94
MRL100C	QSRC	L	5.2	D	447	0.28	101	2423	5413	0.45
MRL50mC	QSRC	L	5.2	W	605	0.12	106	2419	5415	0.45
MRN100C	QSRC	N	16.2	D	447	0.28	100	2433	2400	1.01
MRN50C	QSRC	N	16.2	D	447	0.14	100	2425	2400	1.01
MRN50mC	QSRC	N	20	W	605	0.12	103	2401	5396	0.44
MRNB50mC	QSRC	N	8.9	W	605	0.13	100	2401	5400	0.44
	QSM	Quasi-static Monotonic								
	QSRC	Quasi-static reversed-cyclic								
	DST	Dynamic shake table								

In the first experimental stage of the project Carrillo and Alcocer [2] only square cross-section walls were studied. This stage was divided into monotonic quasi-static tests and cyclical-reversible quasi-static tests. Loading protocol consisted of a series of increasing amplitude cycles. For each increment, two cycles at the same amplitude were applied. During shaking table testing, models were subjected to a series of base excitations represented by earthquake records associated to three limit states. A mass-carrying load system was purposely developed to support the mass and transmit the inertia forces.

Figure 23

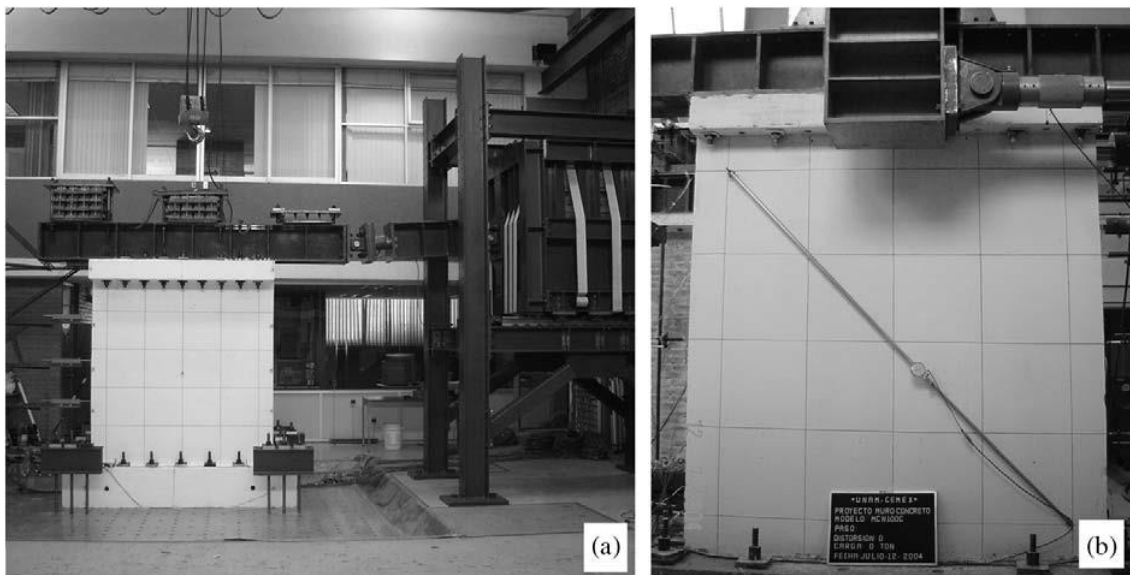


Figure 23. Test setups: (a) shake table testing, (b) quasi-static testing. Source: Carrillo & Alcocer

From the results of the tests. Loads and the correspondent drift values at two different states of the walls were measured: Table 8

- Cracking load  $V_{cr}$ : is defined by the occurrence of the first inclined cracking and distributed over the web of the wall.
- Maximum shear load  $V_{max}$ : The strength limit state is reached.

- Life Safety performance level  $R_{LS}$ : Extension of web inclined cracks to the wall edges without penetrating the boundary elements. [14]
- Ultimate deformation capacity  $V_u$ 
  - When a 20% drop in peak shear strength is observed (walls reinforced with deformed bars).
  - The web shear reinforcement is fractured (web shear reinforcement made of welded-wire).
- $\delta_{cr}$ ,  $\delta_{LS}$  and  $\delta_{max}$ : are the drift ratios associated to the average values of the horizontal displacements at the top section.

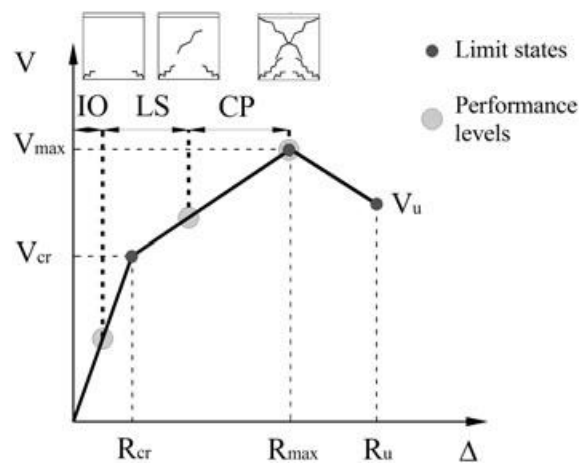


Figure 24. Performance levels and damage states. Source: Acceptance limits for performance-based seismic design of RC walls for low-rise housing. Carrillo and Alcocer.

Table 8. Test results. Carrillo and Alocer

Wall ID	Failure	V <sub>max</sub> (kN)	δ <sub>cr</sub>	δ <sub>LS</sub>	δ <sub>max</sub>
MCL0M	*	*	0.06	0.1	0.44
MCL100C	DC	336	0.12	0.63	0.81
MCL100C-2	DC	336	0.18	0.45	0.8
MCL100D	DT-DC	250	0.14	0.34	0.5
MCL100M	*	*	0.14	0.43	0.98
MCL50C*	*	*	0.07	0.32	0.57
MCL50C-2	DT	375	0.11	0.32	0.58
MCL50M	*	*	0.14	0.43	0.68
MCL50mC	DT	400	0.12	0.32	0.6
MCL50mD	DT	240	0.14	0.35	0.62
MCN0M	*	*	0.1	0.08	0.55
MCN100C	DC-DT	453	0.07	0.28	0.81
MCN100D	DT-DC	274	0.09	0.3	0.53
MCN100M	*	*	0.1	0.42	0.72
MCN50C	DT	352	0.07	0.27	0.66
MCN50C-2	DT	329	0.11	0.21	0.44
MCN50M	*	*	0.1	0.51	1.01
MCN50mC	DT	329	0.11	0.21	0.47
MCN50mD	DT	234	0.09	0.28	0.44
MCNB50mC	*	*	0.05	0.14	0.34
MCS0M	*	*	0.25	0.23	0.73
MCS100C	DT-DC	475	0.23	0.6	1.01
MCS100M	*	*	0.15	0.58	0.97
MCS50C*	*	*	0.13	0.53	1.01
MCS50C-2	DT	321	0.06	0.2	0.39
MEL50mC	DT	172	0.21	0.43	0.7
MEN100C	DC-DT	208	0.24	0.75	1.4
MEN50C	DT	157	0.24	0.67	1.16
MEN50mC	DT	154	0.16	0.39	0.66
MRL100C	*	*	0.1	0.37	0.57
MRL50mC	DT	568	0.05	0.26	0.44
MRN100C	*	*	0.1	0.38	0.6
MRN50C	DT	670	0.1	0.39	0.69
MRN50mC	DT	776	0.03	0.11	0.39
MRNB50mC	DT	612	0.04	0.15	0.4
* No data available					

### 3.2.1.2 Tests by Hidalgo

The response of 26 reinforced concrete shear walls with different height-to-length ratios was tested under cyclic load. Characteristics of the walls are enlisted:

- Height-to-length ratio  $\left(\frac{M}{Vt_w}\right)$ : Varying between 0.35 and 1.0.
- Reinforced concrete shear walls with a rectangular cross-section.
- Concrete compressive strength  $(f'_c)$ : Varying between 15.7 MPa and 24.2 MPa.
- Axial compressive stress  $(\sigma_v)$ : Zero axial compression in the walls except for the weight of the wall and the test setup.
- Web reinforcement  $(f_y)$ : Web reinforcement placed in a single layer at wall mid-thickness.
- Web steel ratio  $\rho$  : The minimum web steel ratio  $(\rho_{min})$  was prescribed by the American Concrete Institute's Building Code (ACI-318 1999).
- Boundary elements: All the walls were designed with enough boundary vertical reinforcement to prevent flexural failure. The thickness of the boundary elements is equal to the thickness  $(t_w)$  of the wall web.

The geometrical and mechanical properties of each specimen are presented in Table 9

Table 9. Wall's geometrical and mechanical properties. Hidalgo

Wall ID	Type of testing	$f_c$ (MPa)	$f_y$ (Mpa)	$\rho_h$ (%)	$\rho_v$ (%)	tw (mm)	hw (mm)	lw (mm)	M/Vlw
1	CHDoIA	19.4	392	0.131	0.251	120	2000	1000	1.00
2	CHDoIA	19.6	402	0.246	0.251	120	2000	1000	1.00
4	CHDoIA	19.5	402	0.381	0.251	120	2000	1000	1.00
6	CHDoIA	17.6	314	0.131	0.259	120	1800	1300	0.69
7	CHDoIA	18.1	471	0.246	0.125	120	1800	1300	0.69
8	CHDoIA	15.7	471	0.246	0.259	120	1800	1300	0.69
9	CHDoIA	17.6	366	0.255	0.255	100	1800	1300	0.69
10	CHDoIA	16.4	367	0.25	0.25	80	1800	1300	0.69
11	CHDoIA	16.3	362	0.127	0.255	100	1400	1400	0.50
12	CHDoIA	17	366	0.255	0.127	100	1400	1400	0.50
13	CHDoIA	18.1	370	0.255	0.255	100	1400	1400	0.50
14	CHDoIA	17.1	366	0.125	0.25	80	1200	1700	0.35
15	CHDoIA	19	366	0.25	0.125	80	1200	1700	0.35
16	CHDoIA	18.8	366	0.25	0.25	80	1200	1700	0.35
21	CHDoIA	24.2	-	0	0	100	1800	1300	0.69
22	CHDoIA	17.2	-	0	0	100	1800	1300	0.69
23	CHDoIA	24.2	431	0.25	0	100	1800	1300	0.69
24	CHDoIA	23.9	431	0	0.25	100	1800	1300	0.69
25	CHDoIA	23.9	-	0	0	100	1400	1400	0.50
26	CHDoIA	17.7	-	0	0	100	1400	1400	0.50
27	CHDoIA	23.9	431	0.25	0	100	1400	1400	0.50
28	CHDoIA	23.3	431	0	0.25	100	1400	1400	0.50
29	CHDoIA	23.2	-	0	0	80	1050	1500	0.35
30	CHDoIA	17.9	-	0	0	80	1050	1500	0.35
31	CHDoIA	23.1	431	0.25	0	80	1050	1500	0.35
32	CHDoIA	23.3	431	0	0.25	80	1050	1500	0.35
Cyclic horizontal displacements of increasing amplitude									

The wall specimens were tested in the test setup shown in Figure 25, which was designed to prevent the rotation of both the top and bottom ends of the specimen while the horizontal cyclic load was applied at the mid-height of the walls. Reinforced concrete blocks were used to attach the test frame to the top and bottom to anchor the specimen.

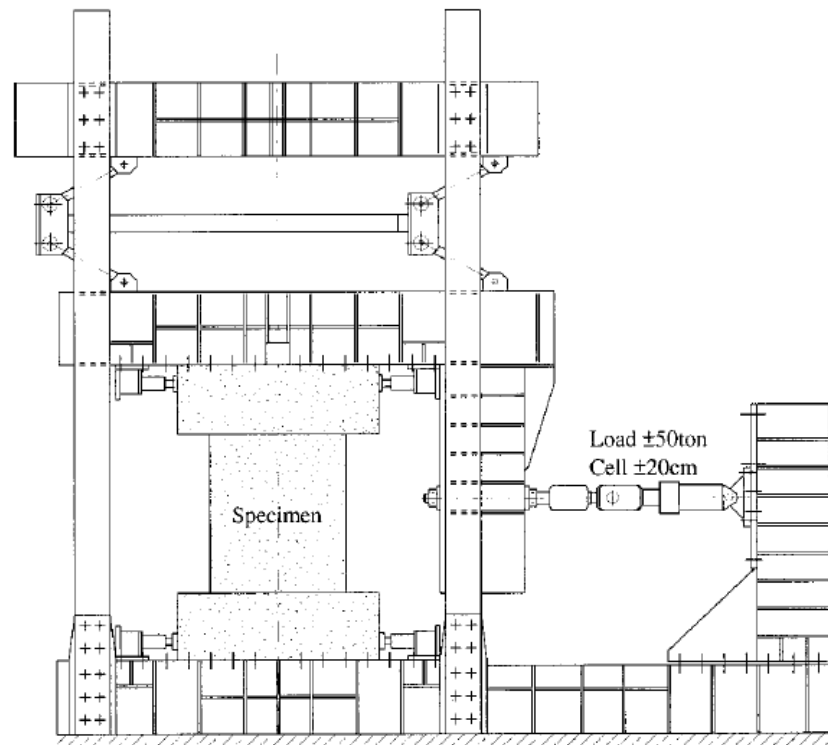


Figure 25. Test setup. Source: Hidalgo

From the results of the test Table 10. Test Results. Hidalgo, loads, and the correspondent drift values at two different states of the walls were measured:

- Cracking load  $V_{cr}$ : is defined as the load at which a change in the slope of the envelope of the load-displacement relationship is observed. The cracking load is generally very close to the load that produced the first diagonal crack from corner to corner of the specimen.
- Maximum shear load  $V_u$ : corresponds to the average value of the maximum shear loads attained in both directions.
- $\delta_{cr}$  and  $\delta_u$ : are the drift ratios associated to the average values of the horizontal displacements at the top section.



Table 10. Test Results. Hidalgo

Wall ID	V <sub>cr</sub>	V <sub>u</sub>	δ <sub>cr</sub> (%)	δ <sub>u</sub> (%)
1	136	198	*	0.66
2	131	270	*	0.75
4	150	324	*	0.75
6	215	309	*	0.44
7	213	364	*	0.63
8	22	374	*	0.55
9	223	258	0.21	0.54
10	116	187	0.1	0.46
11	153	235	0.05	0.35
12	138	304	0.08	0.5
13	144	289	0.05	0.35
14	230	255	0.08	0.25
15	*	368	*	0.42
16	183	62	0.09	0.37
21	162	258	0.11	0.28
22	148	222	0.11	0.27
23	232	333	0.17	0.36
24	173	323	0.12	0.21
25	177	352	0.12	0.6
26	126	262	0.1	0.46
27	244	491	0.2	0.64
28	151	258	0.09	0.31
29	227	400	0.1	0.51
30	159	356	0.06	0.63
31	133	391	0.06	0.35
32	130	344	0.06	0.38

(\*) No data register

### 3.3 Development of fragility functions

#### 3.3.1 Fragility Function Definition

Fragility functions in the FEMA P-58 methodology are statistical distributions that indicate the conditional probability that a component, element, or system will be damaged as a function of a single predictive structural demand parameter, such as story drift or floor acceleration (Figure 26). Fragility functions are typically defined as lognormal cumulative distribution functions, having a median value,  $\theta$ , and logarithmic standard deviation, or dispersion,  $\beta$ . The mathematical form for such a fragility function is: [12]

$$F_i(D) = \phi\left(\frac{\ln\left(\frac{D}{\theta_i}\right)}{\beta_i}\right)$$

- $F_i(D)$ : Is the conditional probability that the wall will be damage to damage state “i” (or a more severe damage state) as a function of story drift ratio (demand parameter).
- $\phi$ : Standard normal (Gaussian) cumulative distribution function.
- $\beta_i$ : Logarithmic standard deviation for damage state “i”, which is determined by the following equation:

- $\beta = \sqrt{\beta_r^2 + \beta_u^2}$

- $\beta_r$ : Is the random variability observed in the test data.
- $\beta_u$ : Represents uncertainty that the tests represent actual conditions of installation and loading or uncertainty that the available data are an adequate sample size to accurately represent the true random variability.

As this study does not meet any uncertainty criteria,  $\beta_u = 0.10$

$$P[i|D] = F_{i+1}(D) - F_i$$

- $P[i|D]$ : Is the conditional probability of exceedance at the Damage State “i”.
- $F_{i+1}$ : Is the conditional probability that the component will be damaged to the damage state “i+1” or a more severe damage state.

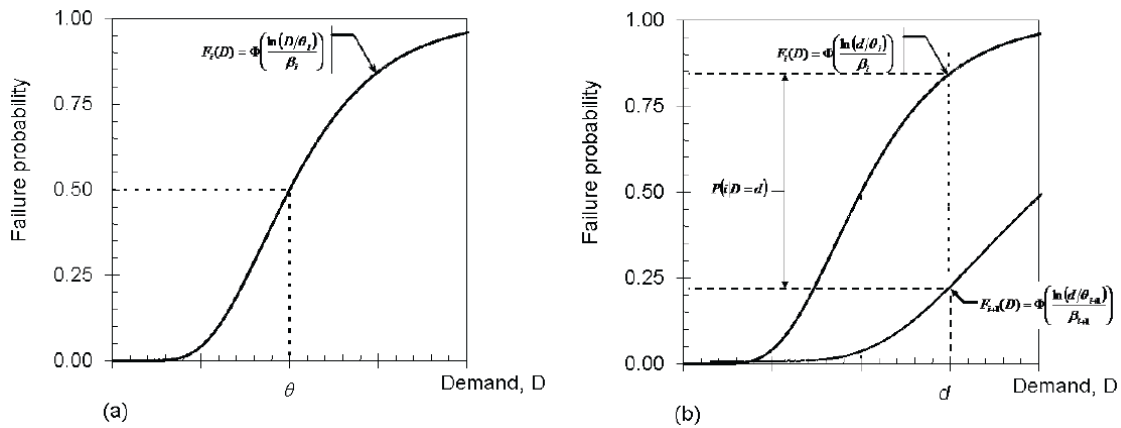


Figure 26. Typical lognormal fragility function (a); and evaluation of individual damage state probabilities (b).  
Source: FEMA P-58-1

### 3.3.2 Derivation of fragility parameters

The drift data presented in section 3.2 has been used for calculating median  $\theta$ , and dispersion  $\beta$ , values for the fragility functions. In this study, the Actual Demand Data described in the FEMA P-58 methodology has been used to this end, as the 61 tests on individual walls provided data to relate exceedance of the different damage state (DS1- Cracking, DS-2-Life Safety, and DS3- Peak Shear Strength) with the drift ratio (demand).

When the damage state is initiated at a known drift ratio ( $d_i$ ), for each wall “i”, the median value of the demand (SDR) which the damage state is likely to initiate ( $\theta$ ) is given by the equation:

$$\theta = e^{\left(\frac{1}{M} \sum_{i=1}^M \ln d_i\right)}$$

- M: total number of walls tested.
- ( $d_i$ ): demand in test “i” at which the damage state was first observed to occur

The value of the random dispersion  $\beta_r$  is given by the following equation:

$$\beta_r = \sqrt{\left(\frac{1}{M-1} \sum_{i=1}^M \left(\ln\left(\frac{d_i}{\theta}\right)\right)^2\right)^2}$$

It is important to remove outliers (a data point with a drift value significantly above or below from the overall data) following the procedures in section H3.2 of FEMA P-58; the values for each damage state are presented in Table 12.

- $\theta$  and  $\beta$ , is calculated for the complete data set.
- D is the number of doubtful observations as shown in Table 11, and R is calculated

from the following equation:  $R = \frac{|\ln(d) - \ln(\theta)|}{\beta}$

- Rmax, is calculated as the maximum value for all the walls in each damage state:

$$|\ln(d_i) - \ln(\theta)|$$

- Eliminate the suspicious measurements if:

$$|\ln(d_i) - \ln(\theta)| > |\ln(d) - \ln(\theta)|_{max}$$

- Obtain  $\theta$  and  $\beta$  for the reduced data set as was done for the original data set.

Table 11. Values of R for applying Peirce's Criterion. Source: FEMA-P-58-VI (2018)

M	D=1	D=2	D=3	D=4	D=5	D=6	D=7	D=8	D=9
3	1.1960								
4	1.3830	1.0780							
5	1.5090	1.2000							
6	1.6100	1.2990	1.0990						
7	1.6930	1.3820	1.1870	1.0220					
8	1.7630	1.4530	1.2610	1.1090					
9	1.8240	1.5150	1.3240	1.1780	1.0450				
10	1.8780	1.5700	1.3800	1.2370	1.1140				
11	1.9250	1.6190	1.4300	1.2890	1.1720	1.0590			
12	1.9690	1.6630	1.4750	1.3360	1.2210	1.1180	1.0090		
13	2.0070	1.7040	1.5160	1.3790	1.2660	1.1670	1.0700		
14	2.0430	1.7410	1.5540	1.4170	1.3070	1.2100	1.1200	1.0260	
15	2.0760	1.7750	1.5890	1.4530	1.3440	1.2490	1.1640	1.0780	
16	2.1060	1.8070	1.6220	1.4860	1.3780	1.2850	1.2020	1.1220	1.0390
17	2.1340	1.8360	1.6520	1.5170	1.4090	1.3180	1.2370	1.1610	1.0840
18	2.1610	1.8640	1.6800	1.5460	1.4380	1.3480	1.2680	1.1950	1.1230
19	2.1850	1.8900	1.7070	1.5730	1.4660	1.3770	1.2980	1.2260	1.1580
20	2.2090	1.9140	1.7320	1.5990	1.4920	1.4040	1.3260	1.2550	1.1900
>20	alnM + b								
a	0.4094	0.4393	0.4565	0.4680	0.4770	0.4842	0.4905	0.4973	0.5046
b	0.9910	0.6069	0.3725	0.2036	0.0701	-0.0401	-0.1358	-0.2242	-0.3079

Table 12. Values for Elimination of Outliers

ID	Damage State	Values of R, for D=1		D	Dmax	Elimination of outliers
		a	b			
DS1	Cracking	0.4094	0.991	2.624090069	2.480838754	Pass
DS2	Life Safety	0.4094	0.991	2.446559496	2.405653405	Pass
DS3	Peak Shear Strength	0.4094	0.991	2.67399176	2.339354895	Pass

Fragility parameters that are developed based on actual demand data should be tested for goodness-of-fit (Lilliefors, 1967):

$$D = \max_x |F_i(d) - S_M(d)|$$

- $S_M(d)$ : is the sample cumulative distribution function

$$S_M(d) = \frac{1}{M} \sum_{i=1}^M H(d_i - d)$$

- $H$ : is taken as 1.0 when  $d_i - d$  is positive

For this study, a value of  $\alpha=0.05$  for the significance level is assigned to rate the fragility function's quality.

- $D_{critical} = \frac{0.895}{M^{0.5} - 0.01 + 0.85M^{-0.5}}$

The values for the goodness-of-fit test for each damage state are presented at

*Table 13. Lilliefors test for Damage States*

ID	Damage State	D critical	D max	Lilliefors test
DS1	Cracking	0.1201	0.1039	Pass
DS2	Life Safety	0.1479	0.0999	Pass
DS3	Peak Shear Strength	0.1132	0.0399	Pass

## 4 Results

### 4.1 Fragility Functions

This study aims to develop a comprehensive set of fragility functions for reinforced concrete shear walls with a shear-controlled behavior, focusing on three distinct damage states: Damage State 1 (slight), Damage State 2 (moderate), and Damage State 3 (severe). The development process adheres to the guidelines provided in the FEMA P-58, as described before, it is ensure a rigorous and standardized approach to quantifying the probability of exceeding each damage state. For all the individual fragility curves,  $\beta = \beta_r$  to show how the lognormal curve adjusts to the empirical data. The results will be presented below:

#### 4.1.1 Damage State 1 (Slight)

As shown in (Table 14), data is available from Carrillo y Alcocer (2012) and Hidalgo (2002) for the story drift ratio of the walls at the specified damage state (slight).

Table 14. Story drift ratio for DS1 (Slight)

#	Author	Wall ID	$\delta_{cr}$ (%)
1	Carrillo & Alcocer	MRN50mC	0.03
2	Carrillo & Alcocer	MRNB50mC	0.04
3	Carrillo & Alcocer	MRL50mC	0.05
4	Carrillo & Alcocer	MCNB50mC	0.05
5	Hidalgo	11	0.05
6	Hidalgo	13	0.05
7	Carrillo & Alcocer	MCL0M	0.06
8	Carrillo & Alcocer	MCS50C-2	0.06
9	Hidalgo	30	0.06
10	Hidalgo	31	0.06
11	Hidalgo	32	0.06
12	Carrillo & Alcocer	MCN50C	0.07
13	Carrillo & Alcocer	MCN100C	0.07

14	Carrillo & Alcocer	MCL50C*	0.07
15	Hidalgo	12	0.08
16	Hidalgo	14	0.08
17	Carrillo & Alcocer	MCN50mD	0.09
18	Carrillo & Alcocer	MCN100D	0.09
19	Hidalgo	16	0.09
20	Hidalgo	28	0.09
21	Carrillo & Alcocer	MCN0M	0.1
22	Carrillo & Alcocer	MCN50M	0.1
23	Carrillo & Alcocer	MCN100M	0.1
24	Carrillo & Alcocer	MRN100C	0.1
25	Carrillo & Alcocer	MRN50C	0.1
26	Carrillo & Alcocer	MRL100C	0.1
27	Hidalgo	10	0.1
28	Hidalgo	26	0.1
29	Hidalgo	29	0.1
30	Carrillo & Alcocer	MCN50mC	0.11
31	Carrillo & Alcocer	MCN50C-2	0.11
32	Carrillo & Alcocer	MCL50C-2	0.11
33	Hidalgo	21	0.11
34	Hidalgo	22	0.11
35	Carrillo & Alcocer	MCL100C	0.12
36	Carrillo & Alcocer	MCL50mC	0.12
37	Hidalgo	24	0.12
38	Hidalgo	25	0.12
39	Carrillo & Alcocer	MCS50C*	0.13
40	Carrillo & Alcocer	MCL50M	0.14
41	Carrillo & Alcocer	MCL100M	0.14
42	Carrillo & Alcocer	MCL50mD	0.14
43	Carrillo & Alcocer	MCL100D	0.14
44	Carrillo & Alcocer	MCS100M	0.15
45	Carrillo & Alcocer	MEN50mC	0.16
46	Hidalgo	23	0.17
47	Carrillo & Alcocer	MCL100C-2	0.18
48	Hidalgo	27	0.2
49	Carrillo & Alcocer	MEL50mC	0.21
50	Hidalgo	9	0.21
51	Carrillo & Alcocer	MCS100C	0.23
52	Carrillo & Alcocer	MEN100C	0.24
53	Carrillo & Alcocer	MEN50C	0.24
54	Carrillo & Alcocer	MCS0M	0.25



The fragility parameters are presented in (Table 15).

Table 15. Fragility parameters for DS1 (Slight)

M	Total number of walls tested	54
$\theta$	Median	0.10
$\beta_r$	Random variability	0.48
$\beta_u$	Uncertainty of the tests	0.10
$\beta$	$\sqrt{\beta_r^2 + \beta_u^2}$	0.49

The fragility curve for Damage state 1 (Slight) is presented in (Figure 27). Note that the lognormal function plotted in this figure includes only random dispersion ( $\beta = \beta_r$ ) to show how the analytical curve adjusts to the empirical data.

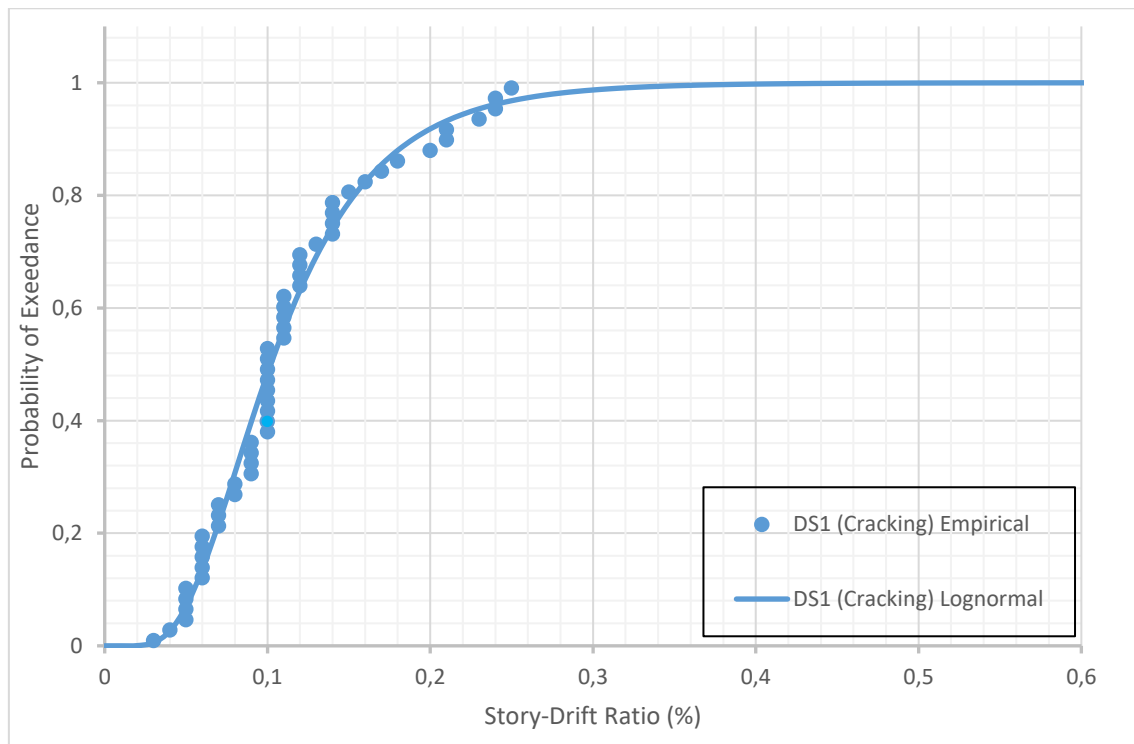


Figure 27. Fragility curve for Damage State 1 (Slight)

#### 4.1.2 Damage State 2 (Moderate)

As shown in (Table 16), data is available from Carrillo y Alcocer (2012). For the experimental study of Hidalgo (2002), no available data or visual information was available to relate the damage state to any given story drift ratio reported.

Table 16. Story drift ratio for DS2 (Moderate)

#	Author	Wall ID	$\delta$ LS (%)
1	Carrillo & Alcocer	MCN0M	0.084
2	Carrillo & Alcocer	MCL0M	0.1
3	Carrillo & Alcocer	MRN50mC	0.11
4	Carrillo & Alcocer	MCNB50mC	0.14
5	Carrillo & Alcocer	MRNB50mC	0.15
6	Carrillo & Alcocer	MCS50C-2	0.2
7	Carrillo & Alcocer	MCN50C-2	0.21
8	Carrillo & Alcocer	MCN50mC	0.21
9	Carrillo & Alcocer	MCS0M	0.23
10	Carrillo & Alcocer	MRL50mC	0.26
11	Carrillo & Alcocer	MCN50C	0.27
12	Carrillo & Alcocer	MCN100C	0.28
13	Carrillo & Alcocer	MCN50mD	0.28
14	Carrillo & Alcocer	MCN100D	0.3
15	Carrillo & Alcocer	MCL50C*	0.32
16	Carrillo & Alcocer	MCL50C-2	0.32
17	Carrillo & Alcocer	MCL50mC	0.32
18	Carrillo & Alcocer	MCL100D	0.34
19	Carrillo & Alcocer	MCL50mD	0.35
20	Carrillo & Alcocer	MRL100C	0.37
21	Carrillo & Alcocer	MRN100C	0.38
22	Carrillo & Alcocer	MEN50mC	0.39
23	Carrillo & Alcocer	MRN50C	0.39
24	Carrillo & Alcocer	MCN100M	0.42
25	Carrillo & Alcocer	MCL100M	0.43
26	Carrillo & Alcocer	MCL50M	0.43
27	Carrillo & Alcocer	MEL50mC	0.43
28	Carrillo & Alcocer	MCL100C-2	0.45
29	Carrillo & Alcocer	MCN50M	0.51
30	Carrillo & Alcocer	MCS50C*	0.53
31	Carrillo & Alcocer	MCS100M	0.58
32	Carrillo & Alcocer	MCS100C	0.6
33	Carrillo & Alcocer	MCL100C	0.63

34	Carrillo & Alcocer	MEN50C	0.67
35	Carrillo & Alcocer	MEN100C	0.75

The fragility parameters are presented in (Table 17)

Table 17. Fragility parameters for DS2 (Moderate)

M	Total number of walls tested	35
$\theta$	Median	0.31
$\beta_r$	Random variability	0.54
$\beta_u$	Uncertainty of the tests	0.10
$\beta$	$\sqrt{\beta_r^2 + \beta_u^2}$	0.55

The fragility curve for Damage State 2 (Moderate) is presented in (Figure 28). Note that the lognormal function plotted in this figure includes only random dispersion ( $\beta = \beta_r$ ) to show how the analytical curve adjusts to the empirical data.

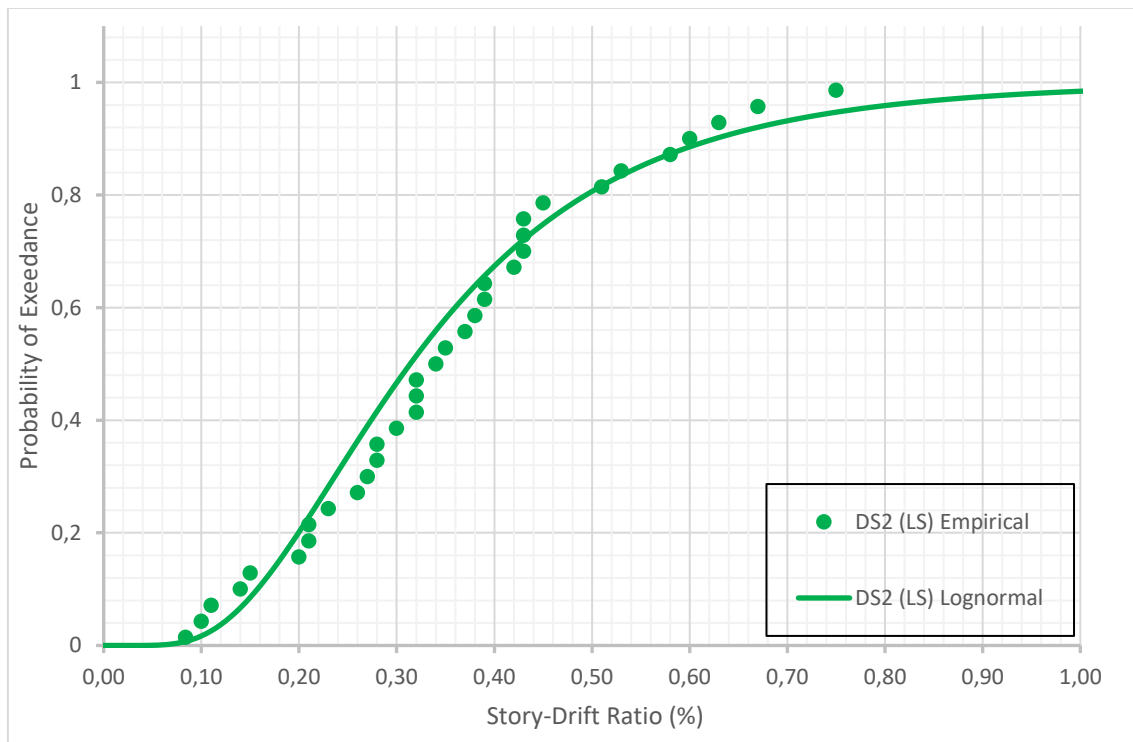


Figure 28. Fragility curve for Damage State 2 (Moderate)

### 4.1.3 Damage State 3 (Severe)

As shown in (Table 18), data is available from Carrillo y Alcocer (2012) and Hidalgo (2002) for the story drift ratio of the walls at the specified damage state (Severe).

Table 18. Story drift ratio for DS3 (Severe)

#	Author	Wall ID	$\delta u$ (%)
1	Hidalgo	24	0.21
2	Hidalgo	14	0.25
3	Hidalgo	22	0.27
4	Hidalgo	21	0.28
5	Hidalgo	28	0.31
6	Carrillo & Alcocer	MCNB50mC	0.34
7	Hidalgo	11	0.35
8	Hidalgo	13	0.35
9	Hidalgo	31	0.35
10	Hidalgo	23	0.36
11	Hidalgo	16	0.37
12	Hidalgo	32	0.38
13	Carrillo & Alcocer	MRN50mC	0.39
14	Carrillo & Alcocer	MCS50C-2	0.39
15	Carrillo & Alcocer	MRNB50mC	0.4
16	Hidalgo	15	0.42
17	Carrillo & Alcocer	MCL0M	0.44
18	Carrillo & Alcocer	MRL50mC	0.44
19	Carrillo & Alcocer	MCN50C-2	0.44
20	Carrillo & Alcocer	MCN50mD	0.44
21	Hidalgo	6	0.44
22	Hidalgo	10	0.46
23	Hidalgo	26	0.46
24	Carrillo & Alcocer	MCN50mC	0.47
25	Carrillo & Alcocer	MCL100D	0.5
26	Hidalgo	12	0.5
27	Hidalgo	29	0.51
28	Carrillo & Alcocer	MCN100D	0.53
29	Hidalgo	9	0.54
30	Carrillo & Alcocer	MCN0M	0.55
31	Hidalgo	8	0.55
32	Carrillo & Alcocer	MCL50C*	0.57
33	Carrillo & Alcocer	MRL100C	0.57
34	Carrillo & Alcocer	MCL50C-2	0.58
35	Carrillo & Alcocer	MRN100C	0.6

36	Carrillo & Alcocer	MCL50mC	0.6
37	Hidalgo	25	0.6
38	Carrillo & Alcocer	MCL50mD	0.62
39	Hidalgo	7	0.63
40	Hidalgo	30	0.63
41	Hidalgo	27	0.64
42	Carrillo & Alcocer	MCN50C	0.66
43	Carrillo & Alcocer	MEN50mC	0.66
44	Hidalgo	1	0.66
45	Carrillo & Alcocer	MCL50M	0.68
46	Carrillo & Alcocer	MRN50C	0.69
47	Carrillo & Alcocer	MEL50mC	0.7
48	Carrillo & Alcocer	MCN100M	0.72
49	Carrillo & Alcocer	MCS0M	0.73
50	Hidalgo	2	0.75
51	Hidalgo	4	0.75
52	Carrillo & Alcocer	MCL100C-2	0.8
53	Carrillo & Alcocer	MCN100C	0.81
54	Carrillo & Alcocer	MCL100C	0.81
55	Carrillo & Alcocer	MCS100M	0.97
56	Carrillo & Alcocer	MCL100M	0.98
57	Carrillo & Alcocer	MCN50M	1.01
58	Carrillo & Alcocer	MCS50C*	1.01
59	Carrillo & Alcocer	MCS100C	1.01
60	Carrillo & Alcocer	MEN50C	1.16
61	Carrillo & Alcocer	MEN100C	1.4

The fragility parameters are presented in (Table 19)

Table 19. Fragility parameters for DS3 (Severe)

NT	Total number of walls tested	61
$\theta$	Median	0.54
$\beta_r$	Random variability	0.39
$\beta_u$	Uncertainty of the tests	0.10
$\beta$	$\sqrt{\beta_r^2 + \beta_u^2}$	0.41

The fragility curve for Damage State 3 (Severe) is presented in (Figure 29). Note that the lognormal function plotted in this figure includes only random dispersion ( $\beta = \beta_r$ ) to show how the analytical curve adjusts to the empirical data.

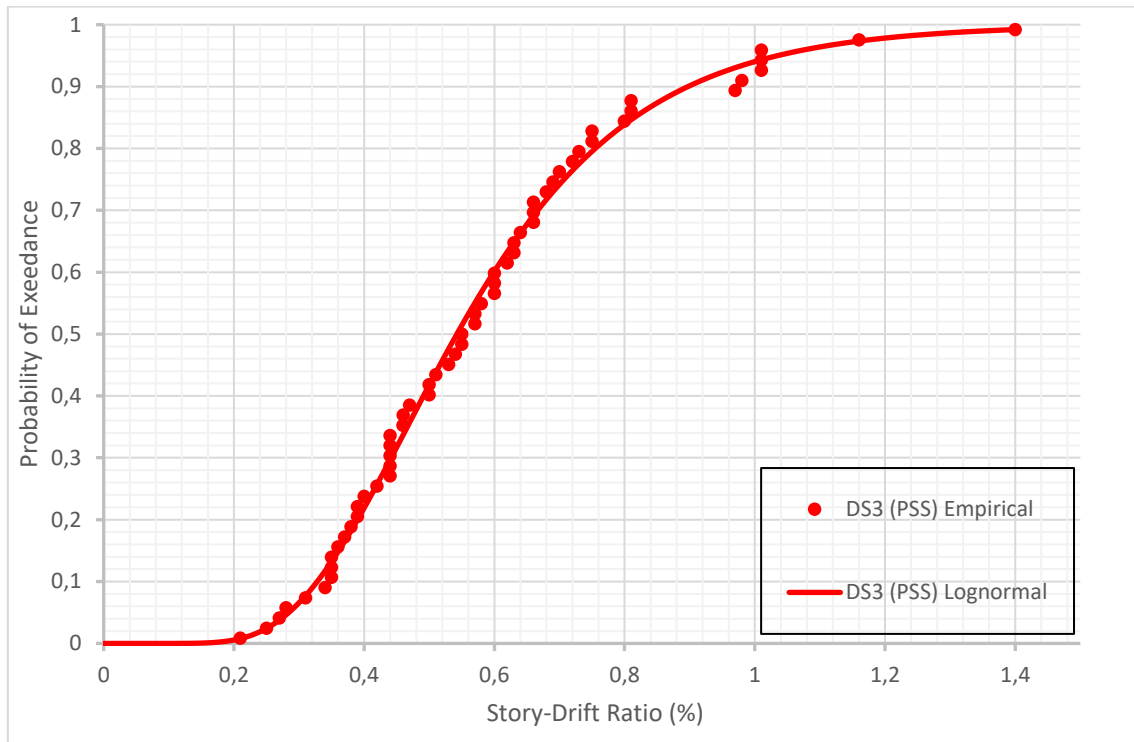


Figure 29. Fragility curve for Damage State 3 (Severe)

## 4.2 Summary and Discussion

The fragility curves of the three damage states, DS1 (Slight), DS2 (Moderate), and DS3 (Severe), are shown in (Figure 30). For this graph,  $\beta = \sqrt{\beta_r^2 + \beta_u^2}$  was considered. In this section, comparisons are also made between the results of the fragility functions and deterministic drift limits (Figure 31) proposed in FEMA 356 (2000) [15], as well as other fragility curves for RC walls proposed by Gulec et al. (2010) [16]

Table 20 presents the lognormal fragility parameters and the corresponding Lilliefors test results for each Damage state. As shown, all the curves pass the Lilliefors test, therefore the lognormal functions adjust well to the empirical data.

Table 20. Lognormal distribution parameters and Lilliefors test

ID	Damage State	$\theta$	$\beta$	D critical	D max	Lilliefors test
DS1	Cracking	0.1021	0.4935	0.1201	0.1039	Pass
DS2	Life Safety	0.3138	0.5479	0.1479	0.0999	Pass
DS3	Peak Shear Strength	0.5425	0.4053	0.1132	0.0399	Pass

### 4.2.1 Comparison with FEMA 356 (2000) drift ratio limits

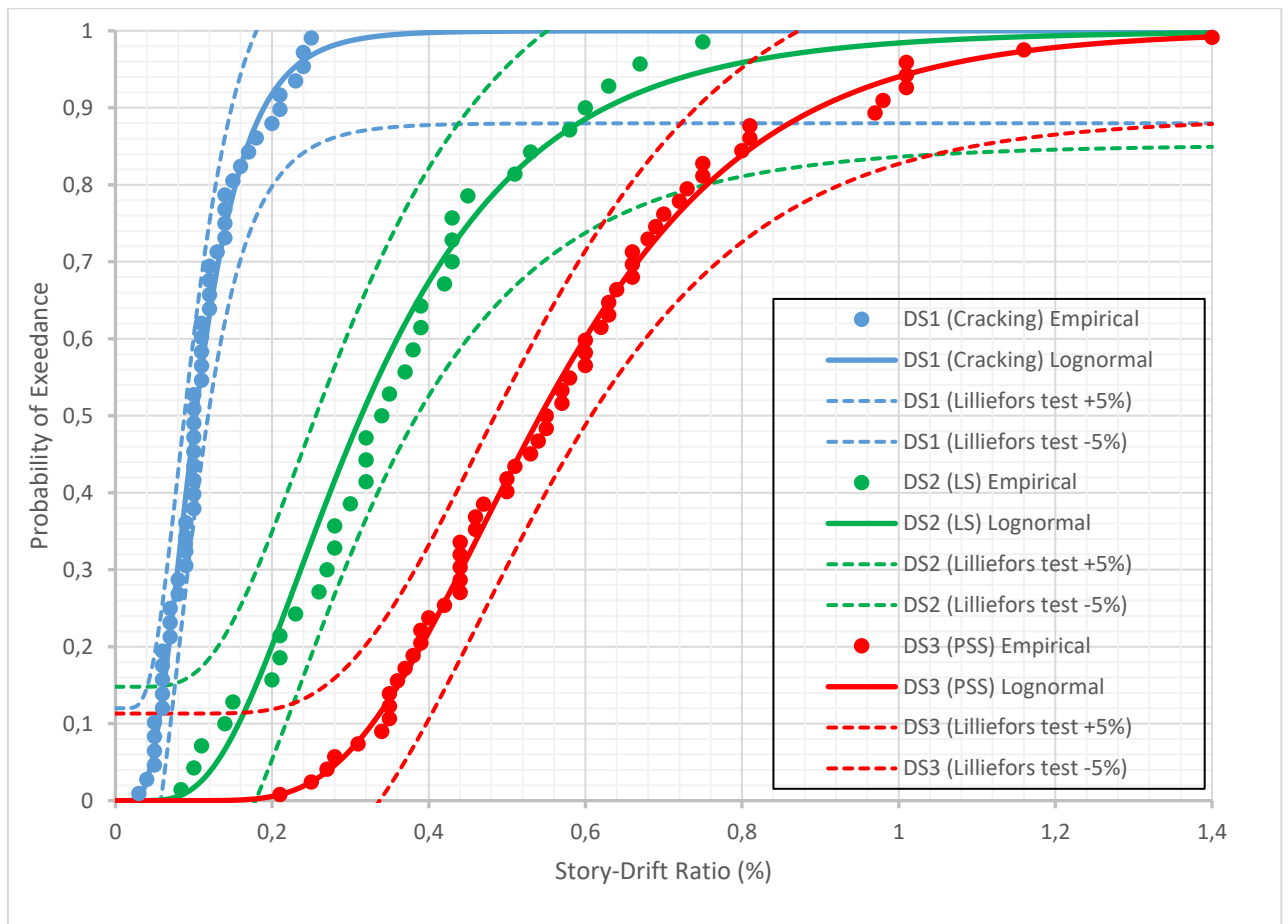


Figure 30. Fragility curves for DS1 (Cracking), DS2 (Life Safety), DS3 (Peak Shear Strength)



**Table 6-19 Modeling Parameters and Numerical Acceptance Criteria for Nonlinear Procedures—Members Controlled by Shear**

Conditions	Total Drift Ratio (%), or Chord Rotation (radians) <sup>1</sup>		Residual Strength Ratio	Acceptable Total Drift (%) or Chord Rotation (radians) <sup>1</sup>				
				Performance Level				
	d	e	c	IO	Component Type			
					Primary		Secondary	
				LS	CP	LS	CP	
<b>i. Shear walls and wall segments</b>								
All shear walls and wall segments <sup>2</sup>	0.75	2.0	0.40	0.40	0.60	0.75	0.75	1.5

1. For shear walls and wall segments, use drift; for coupling beams, use chord rotation; refer to Figures 6-3 and 6-4.  
 2. For shear walls and wall segments where inelastic behavior is governed by shear, the axial load on the member must be  $\leq 0.15 A_g f'_c$ ; otherwise, the member must be treated as a force-controlled component.

Figure 31. Modeling Parameters and Numerical Acceptance Criteria for Nonlinear Procedures - Members Controlled by Shear. Source: FEMA 356 (2000)

The **FEMA 356 (2000)** guidelines propose a series of drift limits to assess the performance of RC walls (Figure 31). The following limits are used:

- Immediate occupancy = 0.40%
- Life safety = 0.60%
- Collapse = 0.75%

To evaluate the fragility curves developed in the present study. These drift values are associated with each Damage State proposed. Table 21 presents the probability of exceedance for each performance level associated with the Damage States.

Table 21. Probability of exceedance for Drift Ratio FEMA 356

Performance level FEMA 356	Drift ratio %	Probability of exceedance (%)		
		DS1 (Slight)	DS2 (Moderate)	DS3 (Severe)
Immediate Occupancy	0.4	100%	67%	22%
Life Safety	0.6	100%	89%	60%
Collapse Prevention	0.75	100%	95%	80%

---

As shown in (Figure 32), the proposed drift for each performance level, Immediate Occupancy, Life Safety, and Collapse Prevention is related to the corresponding Damage States, DS1 (Cracking), DS2 (Life Safety), and DS3 (Peak Shear Strength). The fragility curves show the probability of the exceedance in each Damage State for the defined drift value. For Immediate Occupancy, the probability of exceedance is 100% for DS1, Life Safety is 89%, and Collapse Prevention is 80% for DS3.

Based on this evaluation, the drift values associated with each performance level may be considered relatively high. This suggests that the structural response and potential damage in reinforced concrete shear walls are significant, even under performance levels intended to ensure immediate occupancy or life safety. Considering the types of failure of reinforced concrete walls with low aspect ratio are brittle, and comparing the fragility functions with the story drift values proposed by FEMA 356. We can observe that the damage associated with the fragility functions can be conservative. Conversely, the story drift values are high, given the behavior of squat walls.

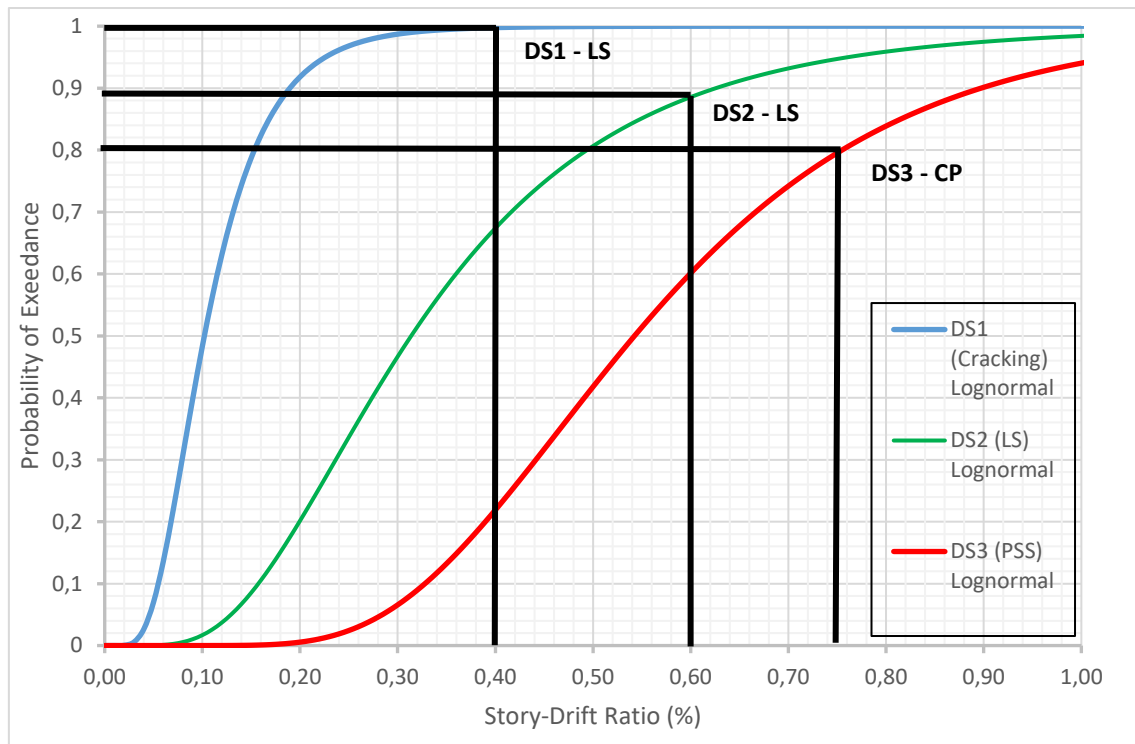


Figure 32. FEMA 356 Drift values and Probability of exceedance for each Damage State

#### 4.2.2 Comparison with fragility functions proposed by Gulec et al. (2010)

The study “Fragility functions for low-aspect-ratio reinforced concrete walls” by Gulec et al. (2010) presents a set of fragility functions for low-aspect-ratio walls, many of them not representing low-rise housing construction but walls for nuclear facilities. Different fragilities are proposed for walls with different cross-sections. Given the interest of this study, only rectangular cross-section walls are to be compared here. Fragility parameters of the functions are presented in (Figure 33) to compare with the fragility functions developed in this study.

ID	Damage states	Method of Repair (MoR)
DS1	Maximum measured crack width less than 0.02 in. (0.5 mm)	Cosmetic repair (MoR-1)
DS2.1	Yielding in web and boundary element reinforcement	Epoxy-resin injection (MoR-2)
DS2.2	Maximum measured crack widths larger than 0.02 in. (0.5 mm) but less than 0.12 in. (3 mm)	
DS2.3	Maximum measured crack widths larger than 0.04 in. (1.0 mm) but less than 0.12 in. (3 mm)	
DS3.1	Concrete crushing at the compression toes/initiation of crushing in the wall web	Partial wall replacement (MoR-3)
DS3.2	Vertical cracking in the toe regions of the web	
DS3.3	Buckling of boundary element vertical reinforcement	
DS3.4	Flexural cracks with widths exceeding 0.12 in. (3 mm)	
DS4.1	Sliding at the base of the wall	Wall replacement (MoR-4)
DS4.2	Wide diagonal cracks	
DS4.3	Widespread crushing of concrete	
DS4.4	Reinforcement fracture	
DS4.5	Shear cracks with widths exceeding 0.12 in. (3 mm)	

Figure 33. Damage states and corresponding methods of repair. Source: Fragility functions for low aspect ratio reinforced concrete walls. Gulec et al. (2010)

Wall geometry	MoR	Lognormal		Lilliefors test results			
		$\theta$	$\beta$	$D_{crit}$	$p$	$H_0$	$D$
Rectangular	1	0.11	0.92	0.110	0.500	A	0.067
	2a	0.43	0.43	0.107	0.028	R	0.113
	2b	0.54	0.36	0.192	0.020	R	0.210
	3	1.03	0.28	0.142	0.214	A	0.116
	4	1.30	0.37	0.134	0.247	A	0.106

Figure 34. Lognormal distribution parameters and the corresponding Lilliefors test results. Source Fragility functions for low aspect ratio reinforced concrete walls. Gulec et al. (2010)

The fragility functions developed for rectangular cross-section walls are shown in Figure

35.

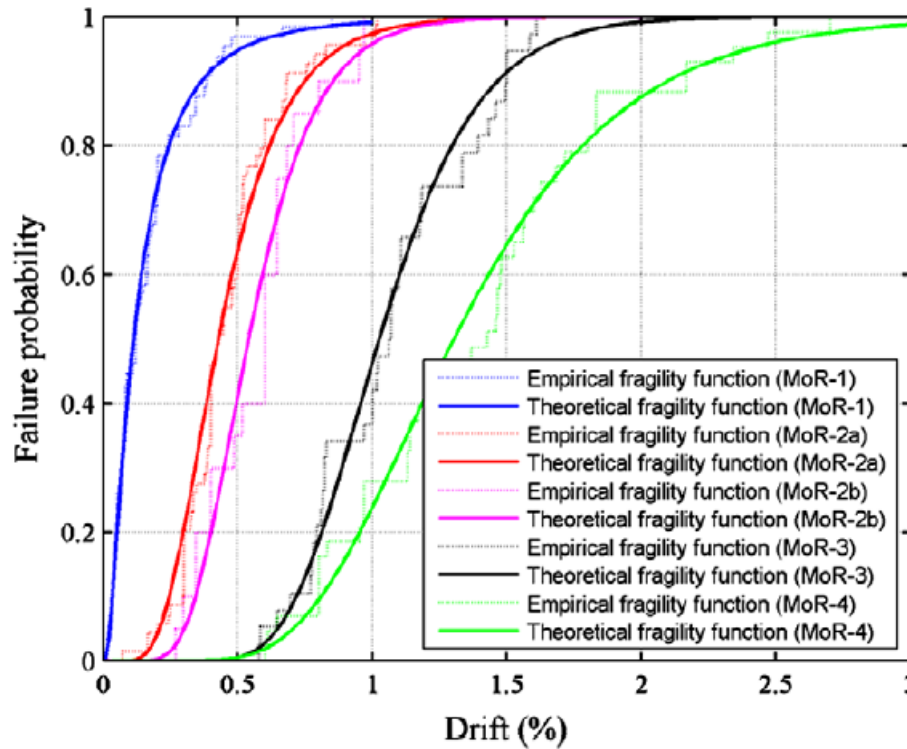


Figure 35. Fragility functions for rectangular walls. Source: *Fragility functions for low aspect ratio reinforced concrete walls*. Gulec et al. (2010)

In both studies, fragility functions are developed for reinforced concrete walls of low aspect ratio with shear-controlled behavior, so geometrical and mechanical properties are similar, but as shown in Table 22, the range of geometric properties in the study made by Gulec is much broader.

Table 22. Geometrical properties for squat walls. Source: Gulec (2009)

Web thickness (mm)	50 - 180
M/Vlw	0.25 - 2.00
Horizontal web reinforcement ratio (%)	0 - 1.5
Vertical web reinforcement ratio (%)	0 - 3.0
Number of web reinforcement layers	1 - 3

Damage State 1 (Cracking) is related to DS1 (Mor-1) of Gulec, where the identification criteria are similar, Occurrence of the first cracking inclined and distributed over the web of the wall and the maximum measured crack width less than 0.5 mm. Also, the method

of repair is the same, Cosmetic repair explained in FEMA 308. Values for  $\theta$  in the present study and in the study of Gulec are 0.10 and 0.11, respectively, and the random variability  $\beta$  are 0.49 and 0.92. This indicates that very similar mean values are obtained, but larger dispersion of results is present in the database of Gulec.

Damage State 2 (Life Safety) is related to DS2.2 (Mor-2) of Gulec, where the identification criteria are similar to the present study, the extension of web-inclined cracks to the wall edges without penetration into the boundary elements and the Maximum measured crack widths larger than 0.5 mm but less than 3 mm. Also, the method of repair is the same, Epoxy-resin injection, as explained in FEMA 308. Values for  $\theta$  in the present study and in Gulec are 0.31 and 0.43, respectively, which indicates that the type of low-rise walls of the present study has a lower deformation capacity for this damage state than those in Gulec. The random variabilities  $\beta$  are 0.55 and 0.43, which indicates that the walls of the present study also present a more uncertain behavior for this damage state.

The major contradiction is in the analysis of Damage State 3 (Peak Shear Strength) that is related to DS3 (Mor-3) of Gulec, where the identification criteria are similar, Noticeable web diagonal cracking and/or yielding of some web steel bars/wires. Moderate web crushing of concrete and damage around openings and Concrete crushing at the compression toes/initiation of crushing in the wall web. Also, the method of repair is similar, Wall Replacement/ Rebar replacement (structural Enhancement), as explained in FEMA 308. The major difference is in Values for  $\theta$  are 0.54 and 1.03, respectively, which indicates that at the Peak Shear Strength of the walls, the damage reported is half the value of the story drift ratio for the fragility functions developed by Gulec et al. (2010) or the walls tested by Carrillo and Alcocer (2012) which indicates that walls for low-rise housing are less resistive to deformation. The random variability  $\beta$  are 0.41 and 0.28,

---

which indicates that the samples for the data developed in both studies tend to suffer close values for story drift values at the expected damage.

## 5 Conclusions

This study focused on the development of damage fragility functions for seismic performance assessment of reinforced concrete wall structures in low-rise housing in Latin America. Consistent with previous guidelines on seismic performance assessment, three damage states were specifically targeted: slight, moderate, and severe. By following the guidelines outlined in FEMA P-58, a rigorous and standardized approach was employed to quantify the probability of exceeding each damage state based on experimental data from wall tests reported in the literature. The development process incorporated various steps, including definition of common geometrical and mechanical wall characteristics of the walls (see Table 23), selection and analysis of relevant test data, definition of damage states and demand parameters, and derivation of fragility functions.

*Table 23. Wall's mechanical and geometrical properties*

Parameter	Typical range	Comment
Height-to-length ratio	0.35 - 2.00	-
Concrete compressive strength (MPa)	15 - 25	-
Web reinforcement	-	Was placed in a single layer at wall mid-thickness.
Web steel ratio (%)	0 -100	The minimum web steel ratio was prescribed by the American Concrete Institute's Building Code ( <b>ACI-318 2011</b> )

The experimental data employed was extracted from studies by Carrillo and Alcocer [2] and Hidalgo [3]. Fragility functions were derived based on this data by establishing a clear relationship between drift ratio (seismic demand) and the likelihood of experiencing each damage state.

The main conclusions of the study are the following:



- Due to the geometric characteristics of the reinforced concrete walls for low-rise construction, their behavior is generally shear controlled and is susceptible to failure modes such as diagonal tension or diagonal compression (web crushing), as reported by Carrillo and Alcocer.

A total of three damage states were considered. DS1 (Slight) occurrence of the first cracking inclined and distributed over the web of the wall, DS2 (Moderate) extension of web-inclined cracks to the wall edges without penetration into the boundary elements, and DS3 (Severe) noticeable web diagonal cracking and/or yielding of some web steel bars/wires. Moderate web crushing of concrete and damage around openings. and the corresponding fragility functions were developed.

- For each damage state, the fragility parameters for the employed lognormal functions are presented in Table 24

*Table 24. Fragility Parameters for Damage States*

		DS1 (Slight)	DS2 (Moderate)	DS3 (Severe)
M	Total number of walls tested	54	35	61
$\theta$	Median drift ratio	0.10%	0.31%	0.54%
$\beta_r$	Random variability	0.48	0.54	0.39
$\beta_u$	Uncertainty of the tests	0.10	0.10	0.10
$\beta$		0.49	0.55	0.41

- Based on the comparison with deterministic drift limits proposed in FEMA 356 for different performance levels, it was found that these limits are unconservative for low-rise housing walls. In specific it was found that at a drift limit for Immediate Occupancy in FEMA 356 the probability of exceeding slight damage was practically 100%; for the Life Safety drift limit the probability of exceeding moderate damage was 89%; and for the Collapse Prevention drift limit the

probability of exceeding severe damage was 80%. This suggests that those drifts are not well suited for this type of walls.

- Comparisons were also made with fragility functions developed by Gulec squat walls with a wider range of characteristics, including those for nuclear facilities. The differences observed in the fragility parameters demonstrates that reinforced concrete walls for low-rise housing have in general a less ductile response than other types of walls. Hence, general fragility functions for walls available in FEMA P-58 might not suit well the behavior of low-rise housing walls.

## 5.1 Recommendations for future works

- Further validation and expansion of fragility functions: Although this study developed fragility functions for shear-controlled reinforced concrete shear walls, additional research is needed to validate these functions using field data and observations from real-world seismic events to enhance the applicability and reliability of the fragility functions.
- Integration of economic and societal considerations: The current study primarily focused on the structural performance of low-rise walls. Future research should incorporate economic and societal considerations to evaluate the potential economic losses, downtime, and social impacts associated with damage states. This holistic approach would enable decision-makers to prioritize mitigation strategies based on a comprehensive understanding of the overall risk.

## 6 References

- [1] M. J. N. Priestley, “Performance-based Seismic Design,” 2000.
- [2] J. Carrillo and S. M. Alcocer, “Backbone model for performance-based seismic design of RC walls for low-rise housing,” *Earthquake Spectra*, vol. 28, no. 3, pp. 943–964, 2012, doi: 10.1193/1.4000068.
- [3] P. A. Hidalgo, C. A. Ledezma, and R. M. Jordan, “Seismic behavior of squat reinforced concrete shear walls,” *pubs.geoscienceworld.org*, 2002, Accessed: Mar. 24, 2023. [Online]. Available: <https://pubs.geoscienceworld.org/earthquake-spectra/article-abstract/18/2/287/584843>
- [4] Applied Technology Council, “Seismic evaluation and retrofit of concrete buildings. Volume 1,” Redwood City, Nov. 1996. [Online]. Available: [www.4downloader.ir](http://www.4downloader.ir)
- [5] FEMA 307, “FEMA 307. Evaluation of Earthquake Damaged Concrete and Masonry Buildings. Technical Resources The Partnership for Response and Recovery,” 1998.
- [6] CENAPRED, “Curso sobre Diseño y Construcción Sismorresistente de Estructuras,” 1999. [Online]. Available: [www.cenapred.unam.mx](http://www.cenapred.unam.mx)
- [7] R. Park, “Ductility evaluation from laboratory and analytical testing,” *iitk.ac.in*, 1988, Accessed: Apr. 12, 2023. [Online]. Available: [http://www.iitk.ac.in/nicee/wcee/article/9\\_vol8\\_605.pdf](http://www.iitk.ac.in/nicee/wcee/article/9_vol8_605.pdf)
- [8] R. Oesterle, A. Fiorato, and L. Johal, “Earthquake resistant structural walls-tests of isolated walls,” *nehrpsearch.nist.gov*, 1976, Accessed: Apr. 14, 2023. [Online]. Available: <https://nehrpsearch.nist.gov/article/PB-271%20467/3/XAB>

- 
- [9] FEMA 306, “FEMA 306. Evaluation of Earthquake Damaged Concrete and Masonry Wall Buildings,” 1998.
- [10] Federal Emergency Management Agency, “FEMA 273. NEHRP Guidelines for the Seismic Rehabilitation of Buildings,” Washington, D.C, Oct. 1997.
- [11] Federal Emergency Management Agency, “FEMA 308. The Repair of Earthquake Damaged Concrete and Masonry Wall Buildings,” 1998.  
<https://mitigation.eeri.org/resource-library/advocacy/the-repair-of-earthquake-damaged-concrete-and-masonry-wall-buildings-fema-308> (accessed Mar. 25, 2023).
- [12] Federal Emergency Management Agency, “FEMA P-58. Seismic Performance Assessment of Buildings Volume 1-Methodology,” 2018. [Online]. Available: [www.ATCCouncil.org](http://www.ATCCouncil.org)
- [13] C. Gulec, “Performance-based assessment and design of squat reinforced concrete shear walls,” 2009, Accessed: Mar. 24, 2023. [Online]. Available: <https://search.proquest.com/openview/200f102091e9bf612d03affe05a755fe/1?pq-origsite=gscholar&cbl=18750>
- [14] J. Carrillo, S. A.-E. engineering & structural, and undefined 2012, “Acceptance limits for performance-based seismic design of RC walls for low-rise housing,” *Wiley Online Library*, vol. 41, no. 15, pp. 2273–2288, 2012, doi: 10.1002/eqe.2186.
- [15] Federal Emergency Management Agency, “FEMA 356. Prestandard and Commentary for the Seismic Rehabilitation of Buildings,” Washington, D.C, Nov. 2000.



- 
- [16] C. Gulec, A. Whittaker, J. H.-E. Structures, and undefined 2010, “Fragility functions for low aspect ratio reinforced concrete walls,” *Elsevier*, vol. 32, pp. 2894–2901, 2010, doi: 10.1016/j.engstruct.2010.05.008.